ADAM10 controls collagen signaling and cell migration on collagen by shedding the ectodomain of discoidin domain receptor 1 (DDR1)

Yasuyuki Shitomi[a], Ida B. Thøgersen[b], Noriko Ito[a], Birgit Leitinger[c], Jan J. Enghild[b], and Yoshifumi Itoh[a]

[a]Kennedy Institute of Rheumatology, Nuffield Department of Orthopaedics, Rheumatology and Musculoskeletal Sciences, University of Oxford, Oxford OX3 7FY, United Kingdom; [b]Department of Molecular Biology and Genetics, University of Aarhus, DK-8000 Aarhus C, Denmark; [c]National Heart and Lung Institute, Imperial College London, London SW7 2AZ, United Kingdom

ABSTRACT **Discoidin domain receptor 1 (DDR1) is a receptor tyrosine kinase that binds and transmits signals from various collagens in epithelial cells. However, how DDR1–dependent signaling is regulated has not been understood. Here we report that collagen binding induces ADAM10-dependent ectodomain shedding of DDR1. DDR1 shedding is not a result of an activation of its signaling pathway, since DDR1 mutants defective in signaling were shed in an efficient manner. DDR1 and ADAM10 were found to be in a complex on the cell surface, but shedding did not occur unless collagen bound to DDR1. Using a shedding-resistant DDR1 mutant, we found that ADAM10-dependent DDR1 shedding regulates the half-life of collagen-induced phosphorylation of the receptor. Our data also revealed that ADAM10 plays an important role in regulating DDR1-mediated cell adhesion to achieve efficient cell migration on collagen matrices.**

Monitoring Editor
Jean E. Schwarzbauer
Princeton University

Received: Oct 21, 2014
Revised: Dec 4, 2014
Accepted: Dec 16, 2014

INTRODUCTION

Extracellular matrix (ECM) is essential in multicellular organisms to maintain functional tissue structures; it acts as scaffolding to support cell migration and as a reservoir for growth factors. In addition, components of ECM can directly transmit signals to cells supporting cell survival and differentiation. Among them, the most abundant ECM component in mammals is collagen, and there are at least five different types of collagen receptors in humans, which include integrins, discoidin domain receptors (DDRs), glycoprotein VI, leukocyte-associated, immunoglobulin-like receptors, and mannose receptors such as Endo180. Among them, DDRs are unique, as they belong to the receptor tyrosine kinase (RTK) family (Leitinger and Hohenester, 2007; Leitinger, 2011).

There are two receptors in this RTK subfamily, DDR1 and DDR2; DDR1 is expressed in epithelial cells primarily, whereas DDR2 is found in mesenchymal cells (Vogel, 1999; Leitinger, 2011). They share ~50% sequence homology, and the common domain structure of DDRs includes a discoidin-homology domain (DD), a discoidin-like domain (DLD), an extracellular juxtamembrane domain, a transmembrane domain, a cytosolic juxtamembrane domain, and a tyrosine kinase domain (TKD). Collagen binding to the DD induces receptor autophosphorylation (Shrivastava *et al.*, 1997; Vogel *et al.*, 1997; Leitinger, 2003), and it has been also shown that Src is involved in DDR1-dependent collagen signaling (Lu *et al.*, 2011). Activation of DDR1 and DDR2 can be induced by different collagens, including type I, II, III, and V collagens, and DDR1 can also be stimulated by type IV collagen (Shrivastava *et al.*, 1997; Vogel *et al.*, 1997). DDRs are believed to play important roles during development, as both DDR1- and DDR2-null mice showed dwarfism, and DDR1-null

This article was published online ahead of print in MBoC in Press (http://www.molbiolcell.org/cgi/doi/10.1091/mbc.E14-10-1463) on December 24, 2014.

Address correspondence to: Yoshifumi Itoh (yoshi.itoh@kennedy.ox.ac.uk).

Abbreviations used: ADAM, a disintegrin and metalloproteinase; CTF, C-terminal fragment; DDR, discoidin domain receptor; DD, discoidin-homology domain; DLD, discoidin-like domain; HEK293, human embryonic kidney 293; IM, ionomycin; MMP, matrix metalloproteinase; MP, metalloproteinase domain; Mst, Marimastat; PI, proteinase inhibitor cocktail; PLA, proximity ligation assay; PY, phosphotyrosine; TCA, trichloroacetic acid; TIMP, tissue inhibitor of metalloproteinases.

mice also showed abnormal development of epithelial organs (Labrador *et al.*, 2001; Vogel *et al.*, 2001). DDRs are also implicated in disease development, including fibrotic disorders of several organs and various cancers (Vogel *et al.*, 2006; Leitinger, 2014). It has been reported that collagen signals mediated by both DDR1 and α2β1 integrin up-regulate N-cadherin expression, which promotes epithelial–mesenchymal transition (Shintani *et al.*, 2008). It has also been reported that DDR1 is an essential transmitter of microenvironmental signals for cell survival, homing, and colonization of lung cancer to promote bone metastasis (Valencia *et al.*, 2012). DDR2 has been implicated in the development of osteoarthritis, as it was shown to be up-regulated in chondrocytes in osteoarthritic cartilage (Xu *et al.*, 2007), and DDR2 activation was shown to induce expression of matrix metalloproteinase 13, which degrades cartilage collagen in osteoarthritis (Xu *et al.*, 2007).

Signaling driven by RTKs must be tightly regulated, since uncontrolled RTK activities would result in tumorigenesis (Porter and Vaillancourt, 1998). To maintain the proper level of RTK signaling in a temporal and spatial manner, at least the following three mechanisms are in place (Blobel, 2005; Dreux *et al.*, 2006; Lemmon and Schlessinger, 2010). First, RTK activation is dependent on its ligand bioavailability. For many RTKs, their ligands are soluble factors and are not present or bioavailable under normal conditions. Expression of the ligands can be induced or the ligands become bioavailable to the RTKs upon different stimuli (Sunnarborg *et al.*, 2002). Thus this regulation of ligand availability for different RTKs is an effective mechanism to control RTK signaling. A second regulation can be endocytosis of the ligand–RTK complex from the cell surface (Marmor and Yarden, 2004; Reiss and Saftig, 2009; Weber and Saftig, 2012; Goh and Sorkin, 2013). This effectively terminates signaling by removing receptors from the cell surface and dissociates ligands from the RTK in endocytic vesicles, followed by intracellular degradation of ligand or receptor molecules or both (Marmor and Yarden, 2004; Goh and Sorkin, 2013). Third, ectodomain shedding of different receptors, including RTKs, can regulate their signaling. This receptor shedding controls the levels of receptor on the cell surface, which is important to maintain signaling levels in check. This can be found in death receptors (Ahonen *et al.*, 2003), Mer tyrosine kinase receptor (Thorp *et al.*, 2011), and fibroblast growth factor receptor 2 (Chan *et al.*, 2012).

Although these regulatory mechanisms are effective in controlling the activity of many of the RTK family members, some of these mechanisms may not be applicable for efficient regulation of DDR signaling because DDR ligands are solid ECM proteins, that is, collagens. Because the collagens are abundantly present in the cellular microenvironment, expression of ligands may not be an effective regulatory step for DDRs. Once DDRs bind to collagen in the solid ECM, DDR–collagen complexes cannot be readily endocytosed. We therefore consider that one way to regulate collagen signaling through DDRs may be shedding of the ectodomain of the receptor. It has been reported that the ectodomain of DDR1 is shed by a metalloproteinase upon collagen stimulation (Vogel, 2002; Slack *et al.*, 2006). However, the responsible sheddase, how shedding is triggered, and, most important, the biological significance of shedding are unknown. Because DDR1 binds to the ECM, it also acts as a cell adhesion molecule, but the relationship between cell adhesion and the shedding event has not been clear.

In this article, we identify a disintegrin and metalloproteinase 10 (ADAM10) as the sheddase responsible for collagen-induced DDR1 shedding. Silencing of the ADAM10 gene abolishes collagen-induced shedding of endogenous or ectopically expressed DDR1. We find that shedding is not a result of DDR1 signaling, but it results from collagen binding to the ectodomain of DDR1. We also show that ADAM10-dependent DDR1 shedding controls the half-life of collagen-induced receptor phosphorylation and is prerequisite for efficient epithelial cell migration on collagen matrices.

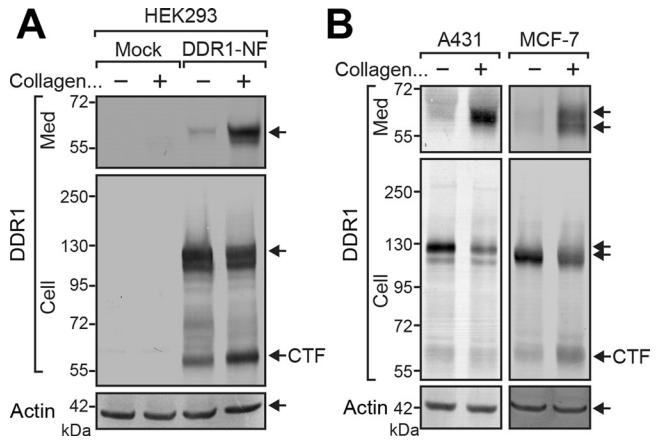

FIGURE 1: Collagen-induced DDR1 ectodomain shedding. (A) HEK293 cells were transiently transfected with empty vector (Mock) or N-terminally FLAG-tagged DDR1 (DDR1-NF) and treated with 100 μg/ml collagen I for 24 h. Conditioned media and cell lysates were analyzed by Western blotting using anti–DDR1 ectodomain (Med), anti–DDR1 C-terminus (Cell), and anti-actin (actin) antibodies. CTF, C-terminal fragment. (B) A431 and MCF-7 cells were incubated for 24 h in the presence or absence of collagen I. Conditioned media and cell lysates were analyzed as in A. Arrows point to detected protein bands for shed DDR1, full-length DDR1, CTF, and actin.

RESULTS

Collagen induces shedding of the DDR1 ectodomain by a metalloproteinase

To investigate collagen-induced ectodomain shedding of DDR1, we transiently transfected human embryonic kidney 293 (HEK293) cells with an expression plasmid for N-terminally FLAG-tagged DDR1 (DDR1-NF) or mock vector, and stimulated them with collagen I. After 24 h, a significant amount of the shed form of DDR1-NF with a molecular size of 60 kDa was detected in the conditioned medium of collagen-treated cells, which was accompanied by reduced levels of 120-kDa, full-length DDR1 and increased levels of the receptor remnant, the so-called C-terminal fragment (CTF), in comparison to untreated cells (Figure 1A). Collagen-induced DDR1 shedding was also confirmed in cells expressing endogenous DDR1, including A431 squamous cell carcinoma and MCF-7 human breast carcinoma cell lines (Figure 1B). The molecular size of full-length and shed DDR1 in MCF-7 was slightly lower than that in A431, which might be the result of different posttranslational modifications such as glycosylation or expression of different DDR1 isoforms. We observed two shed fragments of DDR1 in the medium of MCF-7 upon collagen stimulation. The reason for the appearance of the two forms of shed DDR1 in MCF-7 cells is not clear. We also detected minor spontaneous DDR1 shedding without collagen stimulation (Figure 1, –Collagen), but collagen-induced DDR1 shedding occurred at significantly higher levels. The appearance of the CTF is inconsistent between the cell lines, which may be attributed to different levels of clearance of the CTF during the 24-h period of culture. Taken together, these results suggest that collagen-induced DDR1 shedding is likely to be a common property of DDR1-expressing cells.

To search for a potential proteinase involved in DDR1 ectodomain shedding, we examined the effect of inhibitors for different

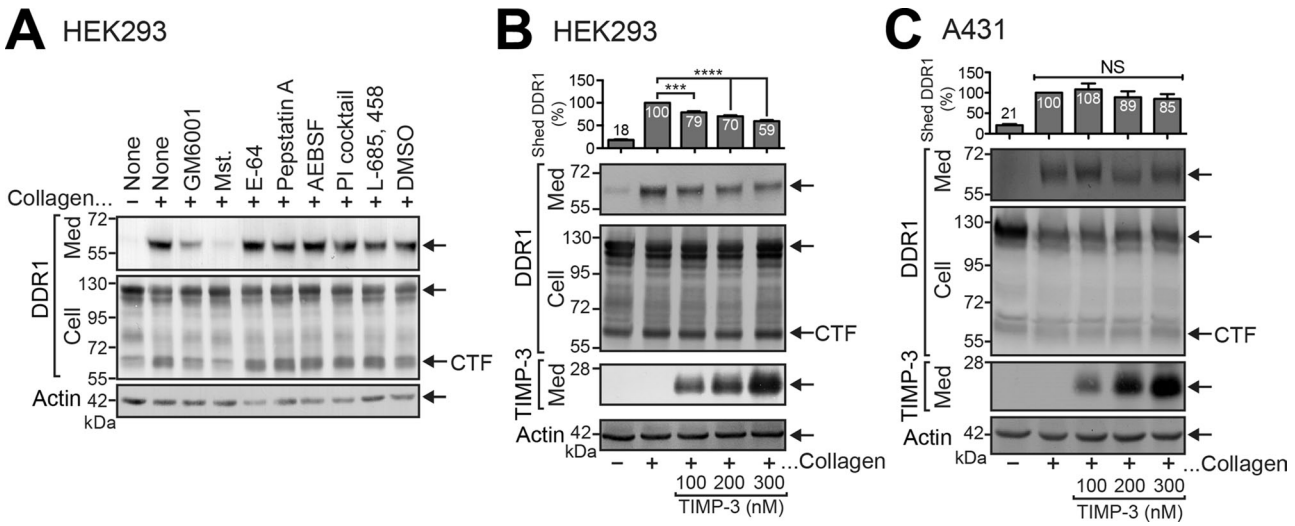

FIGURE 2: The sheddase responsible for collagen-induced DDR1 shedding is TIMP-insensitive. (A) HEK293 cells were transiently transfected with DDR1-NF and treated with collagen I for 24 h in the presence or absence of 10 μM GM6001, 10 μM Mst, 10 μM E-64, 10 μM pepstatin A, 100 μM AEBSF, PI cocktail, 1 μM γ-secretase inhibitor X (L-685, 458), or vehicle control (DMSO). Conditioned media and cell lysates were subjected to Western blotting using anti–DDR1 ectodomain (Med), anti–DDR1 C-terminus (Cell), or anti-actin antibodies. CTF, C-terminal fragment. (B, C) HEK293 cells transiently transfected with N-terminally FLAG-tagged DDR1 (B) and A431 (C) cells were treated for 24 h with serum-free DMEM containing 100 μg/ml collagen I in the presence or absence of TIMP-3 at a concentration of 100, 200, or 300 nM. Conditioned media and cell lysates were analyzed by Western blotting using anti–DDR1 ectodomain (Med), anti–DDR1 C-terminus (Cell), anti-FLAG (TIMP-3, Med), or anti-actin antibodies. The band intensity of shed DDR1 was analyzed with Phoretix and standardized by the intensity of shed DDR1 in collagen-treated medium. Data shown at the top represent the means ± SEM. $N = 3$ for each condition. ***$p < 0.005$; ****$p < 0.0001$; NS, not significant ($p > 0.05$; one-way analysis of variance [ANOVA]) compared with collagen-treated medium.

classes of proteinases, including metalloproteinase inhibitors GM6001 and Marimastat (Mst), a cysteine proteinase inhibitor (E-64), an aspartic proteinase inhibitor (pepstatin A), a serine proteinase inhibitor (AEBSF), and a γ-secretase inhibitor X (L-685, 458). Among them, only the broad-spectrum metalloproteinase inhibitors GM6001 and Mst inhibited shedding of DDR1 (Figure 2A), confirming that a metalloproteinase is responsible, as previously reported (Vogel, 2002). To characterize further metalloproteinase activity, we examined the effect of tissue inhibitor of metalloproteinase-1 (TIMP-1), TIMP-2, and TIMP-3 on DDR1 shedding. We found that addition of TIMP-1 or TIMP-2 at 500 nM did not influence the shedding in HEK293 cells and A431 cells (Supplemental Figure S1, A and B). It was reported that overexpression of TIMP-3 inhibited DDR1 shedding by 75% in HEK293 cells (Slack *et al.*, 2006). Our data also showed that addition of purified TIMP-3 at 100, 200, and 300 nM partially inhibited DDR1 shedding in HEK293 cells by 21, 30, and 41%, respectively (Figure 2B). We also examined effects of both stable and transient expression of TIMP-3 in HEK293. However, TIMP-3 overexpression did not inhibit DDR1 shedding in our experimental conditions (Supplemental Figure S1, B and C). We speculate that this lack of inhibition may be due to insufficient levels of TIMP-3 produced from those transfected cells. These results suggest that DDR1 shedding can be inhibited by TIMP-3, but it requires high concentration for inhibition of DDR1 shedding in the HEK293 cell system. To examine whether this is also the case for endogenous DDR1 shedding, we analyzed the effect of TIMP-3 in A431 cells. In contrast to HEK293 cells, endogenous DDR1 shedding was not inhibited by TIMP-3 even at 300 nM (Figure 2C). We were unable to examine a higher concentration of TIMP-3 due to the difficulty of TIMP-3 purification. The inability of TIMP-3 to inhibit DDR1 shedding was unlikely due to loss of bioavailability of TIMP-3, which can be caused by its endocytosis through LRP1 (Scilabra *et al.*, 2013), as significant amounts of TIMP-3 (~80% remained for each concentration of TIMP-3) were detected in the medium even after 24 h of incubation (Figure 2C). We thus concluded that collagen-induced endogenous DDR1 shedding is insensitive to TIMPs, including TIMP-3 in A431 cells.

ADAM10 knockdown abrogated DDR1 ectodomain shedding upon collagen stimulation

Our data indicated that the enzyme responsible for collagen-induced DDR1 shedding is a metalloproteinase insensitive to TIMP-1 and TIMP-2 and partially sensitive or insensitive to TIMP-3 (Figure 2, B and C). It has been shown that TIMP-insensitive metalloproteinases include ADAM8, ADAM9 (Amour *et al.*, 2002), and ADAM19 (Chesneau *et al.*, 2003; Shiomi *et al.*, 2010). We therefore knocked down ADAM8, ADAM9, and ADAM19, along with well-characterized sheddases, ADAM10 and ADAM17, in A431 cells. The mRNA levels of each ADAM in the respective siRNA treated cells were significantly down-regulated compared with the nontargeting small interfering RNA (siRNA; si-NT)–treated cells by 60% (ADAM8), 86% (ADAM9), 95% (ADAM10), 89% (ADAM17), and 99% (ADAM19; Figure 3A). Under these conditions, only ADAM10 knockdown abolished collagen-induced DDR1 shedding (Figure 3A, DDR1, Med). It was noted that although Mst and ADAM10 knockdown inhibited shedding of DDR1, cellular level of DDR1 did not recover to the level of non–collagen-treated cells in A431 cells (Figure 3A). This is likely due to down-regulation of DDR1 production upon collagen treatment during 24-h incubation. We also confirmed the effect of ADAM10 knockdown in MCF-7 (Supplemental Figure S2) and HEK293 cells (see later discussion of Figure 7E, WT). Recently it was reported that overexpression of

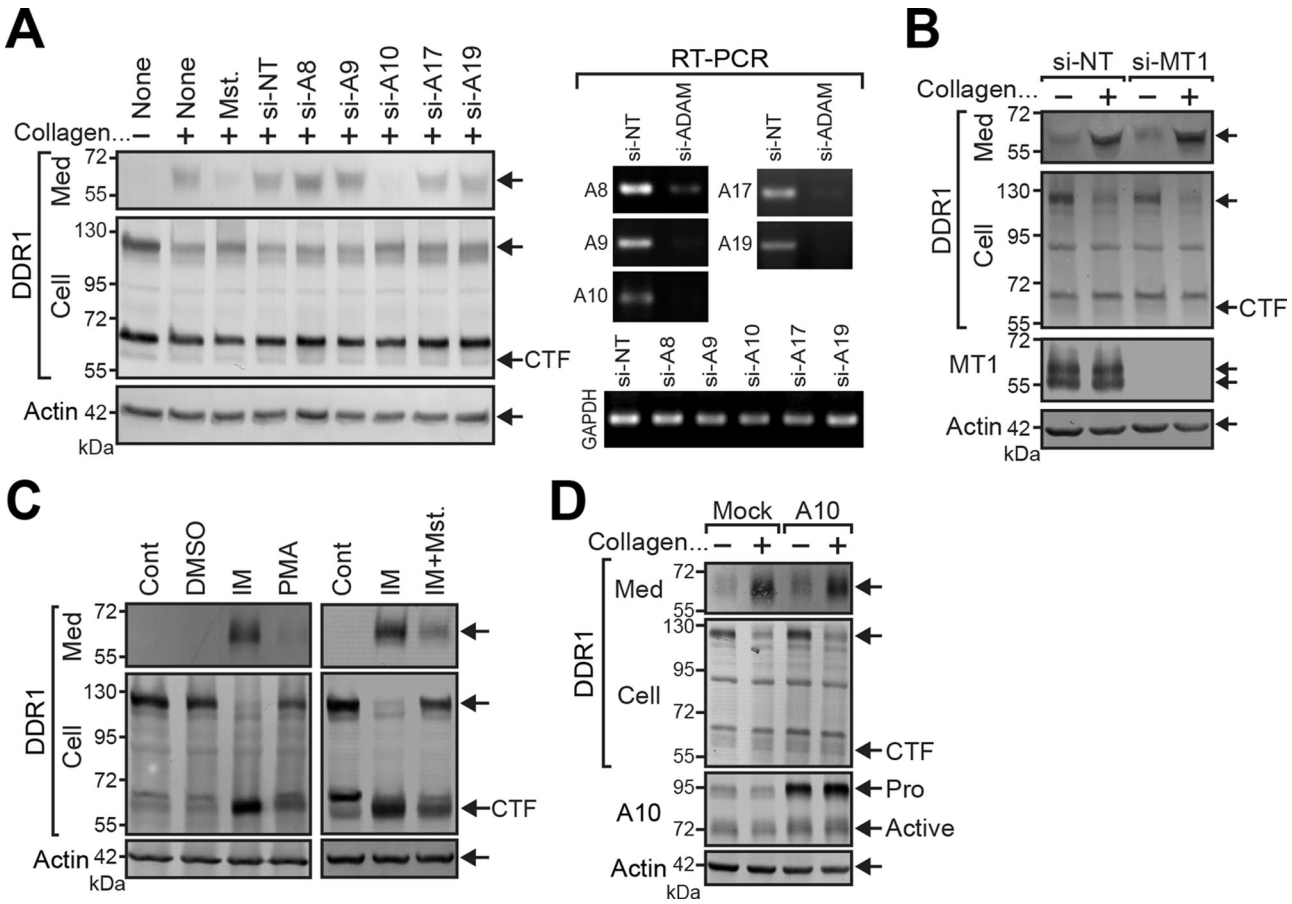

FIGURE 3: ADAM10 is the sheddase responsible for collagen-induced DDR1 ectodomain shedding. (A) A431 cells were transfected with siRNA for ADAM8, ADAM9, ADAM10, ADAM17, or ADAM19 or with nontargeting (NT) siRNA. After 48 h, cells were treated with collagen I (100 μg/ml) for a further 24 h. We confirmed that the level of mRNA for each enzyme was reduced by 60–99% after 72 h (right, RT-PCR). Mst (10 μM) was used as a positive control for inhibition of DDR1 shedding. Conditioned media and cell lysates were analyzed by Western blotting using anti–DDR1 ectodomain (Med), anti–DDR1 C-terminus (Cell), or anti-actin antibodies. Note that ADAM10 knockdown resulted in inhibition of endogenous DDR1 shedding. CTF, C-terminal fragment. (B) A431 cells were transfected with siRNA for MT1-MMP (si-MT1) or si-NT. Cells were then treated with collagen I for 24 h. Conditioned media and cell lysates were analyzed by Western blotting using anti-DDR1, anti-MMP14 (EP1264Y) (MT1), and anti-actin antibodies. (C) A431 cells were treated with 1 μM IM, 25 ng/ml PMA, or DMSO vehicle control (0.001%) for 1 h. Conditioned media and cell lysates were analyzed as in A. A431 cells were also treated with 1 μM IM for 1 h in the presence or absence of 10 μM Mst (right). (D) A431 cells were transiently transfected with ADAM10 or mock vector and treated with or without collagen I for 24 h. Conditioned media and cell lysates were subjected to Western blotting using anti–DDR1 ectodomain (Med), anti–DDR1 C-terminus (Cell), anti-ADAM10 (A10), and anti-actin antibodies.

MT1-matrix metalloproteinase (MMP) induced spontaneous DDR1 shedding in COS1 cells and T47D breast cancer cells, although the authors could not confirm a role of endogenous MT1-MMP as a constitutive DDR1 sheddase in HCC1806 breast cancer cell (Fu *et al.*, 2013). Because A431 cells express endogenous MT1-MMP along with endogenous DDR1, we next examined whether MT1-MMP is involved in DDR1 shedding in our experimental setting. As shown in Figure 3B, knockdown of MT1-MMP in A431 cells did not affect spontaneous or collagen-induced DDR1 shedding, suggesting that MT1-MMP is not involved in DDR1 shedding in A431 cells, supporting the data on HCC1806 in the report by Fu *et al*. (2013). MT1-MMP is expressed in neither HEK293 nor MCF7 cells (unpublished data). Thus MT1-MMP is unlikely to be involved in DDR1 shedding in our experimental conditions.

Because ADAM10-dependent shedding of different cell surface molecules can be activated by calcium ionophores (Le Gall *et al.*, 2009), we examined the effect of ionomycin (IM). As shown in Figure 3C, DDR1 shedding in A431 was induced by IM treatment, whereas the phorbol ester (phorbol 12-myristate 13-acetate [PMA]) had no effect. Addition of Mst or ADAM10 knockdown inhibited the IM-induced DDR1 shedding by 83 and 54%, respectively (Figure 3C and Supplemental Figure S3). We next examined whether ectopic expression of ADAM10 can induce DDR1 shedding in A431 cells (Figure 3D). Expression of ADAM10 resulted in a 1.9-fold increase of the active form of ADAM10 compared with mock-transfected cells, but it did not induce DDR1 shedding in nonstimulated cells and did not influence collagen-induced DDR1 shedding (Figure 3D). This suggests that excess ADAM10 does not induce or contribute to DDR1 shedding. Taking the results together, we identified ADAM10 as a responsible DDR1 sheddase, but this process is only weakly sensitive to TIMP-3: it requires high concentrations of TIMP-3 (≥300 nM), despite the fact that ADAM10 is sensitive to TIMP-1 and TIMP-3 inhibition (Amour *et al.*, 2000).

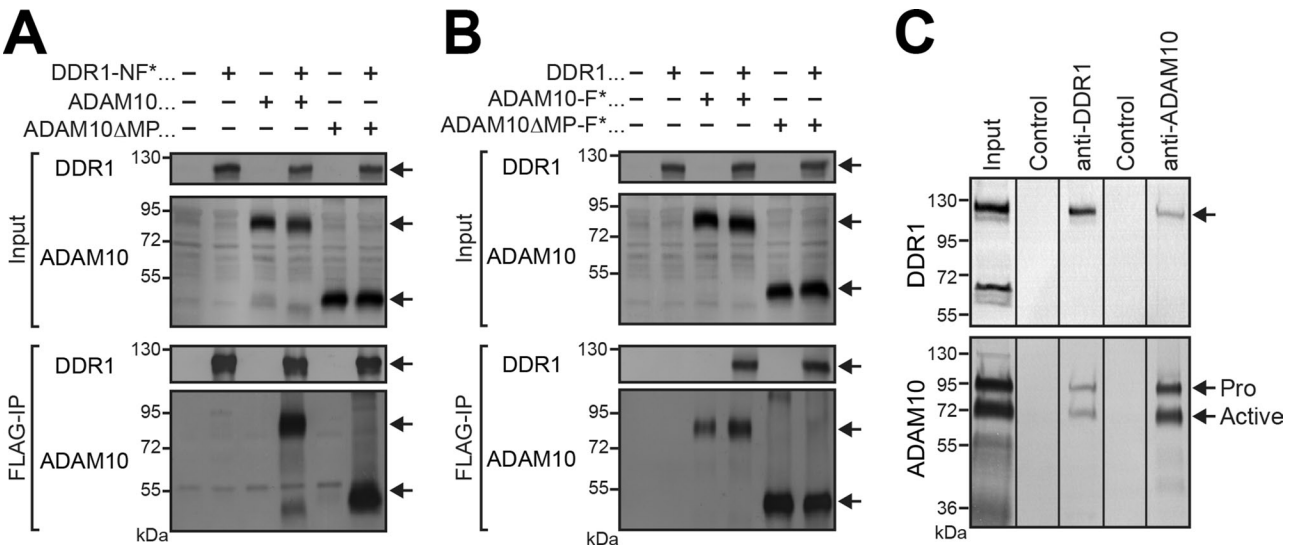

FIGURE 4: Coimmunoprecipitation of DDR1 with ADAM10. (A) HEK293 cells were cotransfected with DDR1-NF, wild-type ADAM10, or ADAM10ΔMP in combination as indicated and subjected to immunoprecipitation with anti-FLAG affinity beads. Bound materials were analyzed by Western blotting using anti–DDR1 ectodomain or anti-ADAM10 antibodies. Asterisks indicate the protein that was pulled down. MP, metalloproteinase domain. (B) HEK293 cells were transiently cotransfected with FLAG-tagged ADAM10 (ADAM10-F), ADAM10ΔMP-F, or DDR1 in combination as indicated. Cell lysates were immunoprecipitated with anti-FLAG antibody, followed by Western blotting with anti-DDR1 ectodomain or anti-ADAM10 antibodies. DDR1 was coimmunoprecipitated with ADAM10-F or ADAM10ΔMP-F (FLAG-immunoprecipitation, top). Asterisks indicate the protein that was pulled down. (C) Coimmunoprecipitation of endogenous DDR1 and ADAM10. A431 cells were subjected to cell surface biotinylation before cell lysis. Cell lysates were subjected to two-step affinity precipitation using antixDDR1 ectodomain or anti-ADAM10 ectodomain conjugated to protein G–coated Dynabeads followed by streptavidin beads. Coimmunoprecipitated DDR1 and ADAM10 bound to streptavidin beads were visualized by Western blotting using anti-DDR1 C-terminus or anti-ADAM10 antibodies. Control sample was incubated with protein G–Dynabeads without antibodies. Active, active form of ADAM10; Pro, proform. Blank lanes that were cropped out of the blot are indicated by black lines.

DDR1 interacts with ADAM10 on the cell surface

We postulated that a potential reason for weak sensitivity of ADAM10-dependent DDR1 shedding to TIMP-3 inhibition may be due to steric hindrance caused by complex formation between ADAM10 and DDR1. To examine this possibility, we cotransfected HEK293 cells with DDR1-NF and nontagged ADAM10 and subjected the cell lysates to coimmunoprecipitation using anti-FLAG beads. As shown in Figure 4A (FLAG-immunoprecipitation, bottom), ADAM10 was coimmunoprecipitated with DDR1-NF. A similar result was obtained by coimmunoprecipitation of DDR1 with FLAG-tagged full-length ADAM10 (ADAM10-F) or ADAM10-F without metalloproteinase domain (ADAM10ΔMP-F; Figure 4B), suggesting that ADAM10 is indeed in a complex with DDR1, and the catalytic metalloproteinase domain of ADAM10 is not essential for this interaction. We next investigated whether endogenous ADAM10 can form a complex with endogenous DDR1 in A431 cells. In these experiments, A431 cells were surface biotinylated before lysis of the cells and subjected to immunoprecipitation using anti-DDR1 antibody or anti-ADAM10 antibody. This two-step affinity precipitation, which involves initial precipitation with anti-DDR1 or anti-ADAM10 followed by streptavidin beads, allowed us to detect cell surface complexes of DDR1 and ADAM10. As shown in Figure 4C (Input, bottom), both proADAM10 and active ADAM10 were detected in A431 cells. The data indicate that both proform and active form of ADAM10 were coimmunoprecipitated with endogenous DDR1, suggesting that endogenous ADAM10 and DDR1 form a complex on the cell surface.

We next examined the interaction between DDR1 and ADAM10 on the cell surface using in situ proximity ligation assay (PLA). PLA highlights two molecules within 40 nm of each other. As shown in Figure 5A, a bright PLA signal was detected in HEK293 cells stably expressing DDR1-NF, suggesting that DDR1 was indeed in a complex with endogenous ADAM10 on the cell surface. Some PLA signals were also detected in mock cells (Figure 5A, Mock). This is most likely due to expression of low levels of endogenous DDR1 in HEK293 cells. We next examined interaction of endogenous DDR1 and ADAM10 in A431 cells, using PLA (Figure 5B). Bright PLA signal was detected on the cell surface of A431 cells without collagen treatment, and the signals were notably reduced upon collagen treatment. This suggests that most of DDR1 in complex with ADAM10 has been shed and dissociated from ADAM10. The reduction of the signal was completely prevented by addition of Mst (Figure 5B, +Coll+Mst), supporting this notion. Although it is not clear whether ADAM10 and DDR1 directly interact with each other, these data suggest that they are at least in the same molecular complex on the cell surface.

Collagen binding, but not DDR1 signaling, is required for DDR1 ectodomain shedding

There are two potential mechanisms to explain collagen-induced shedding of DDR1. First, collagen-induced DDR1 signaling may trigger the functional activation of ADAM10 (Vogel, 2002); second, the orientation of DDR1 may be altered upon collagen binding, which allows ADAM10 to cleave DDR1. We first investigated whether collagen-induced DDR1 signaling plays a role. We used a kinase-dead mutant of DDR1 (DDR1-KD) and a cytoplasmic domain

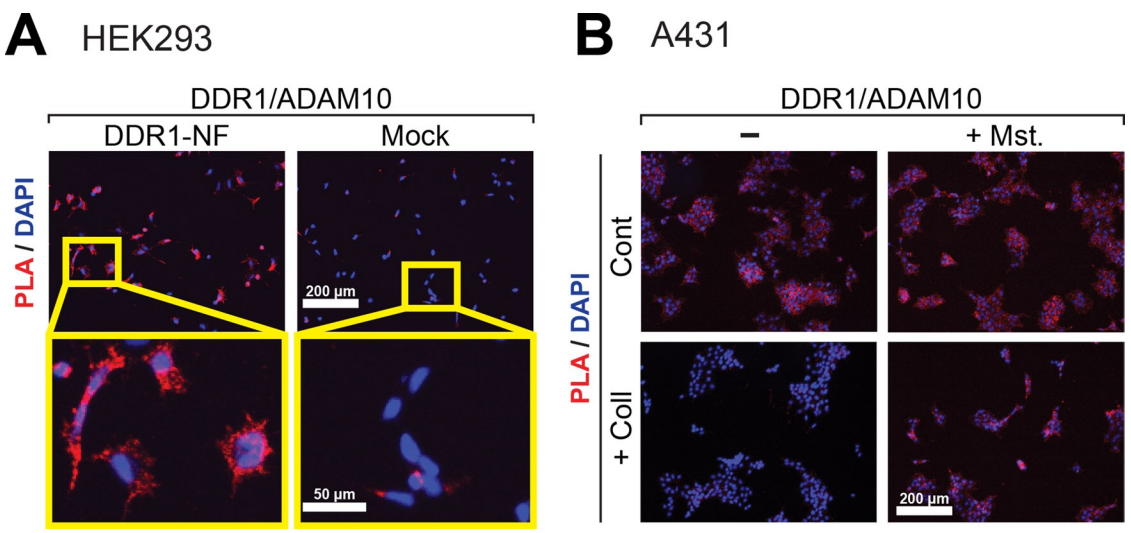

FIGURE 5: DDR1 is in a complex with ADAM10 on the cell surface. (A) HEK293 cells stably expressing DDR1-NF were subjected to PLA using anti–DDR1 ectodomain and anti-ADAM10 ectodomain antibodies. The PLA signal is shown in red. Nuclei were stained with DAPI (blue). Scale bars, 200 and 50 μm. (B) A431 cells were stimulated with collagen I for 24 h in the presence or absence of 10 μM Mst and subjected to PLA as in A. Scale bar, 200 μm.

deletion mutant (DDR1ΔC), both of which are not able to transmit collagen signals (Figure 6A). We confirmed that those mutants are expressed on the cell surface in a similar manner to wild-type (WT) DDR1 by a surface biotinylation assay (Supplemental Figure S4A). As shown in Figure 6B, upon collagen stimulation, the ectodomain of DDR1-KD and DDR1ΔC was shed in an efficient manner. We also examined the effect of a tyrosine kinase inhibitor, dasatinib, which inhibits DDR1 with an IC_{50} of 1.35 nM (Day *et al.*, 2008). As shown in Figure 6C, dasatinib treatment at 50 nM did not influence DDR1 shedding, whereas it completely inhibited phosphorylation of DDR1 upon collagen stimulation. These data strongly suggest that collagen-induced DDR1 shedding is not dependent on DDR1 signaling.

Next we investigated whether binding of collagen to the DDR1 ectodomain is required for its shedding. For these experiments, we used a DDR1 mutant, R105A (Figure 6A). This mutation in the DD of DDR1 was shown to abrogate binding of the receptor to collagen (Abdulhussein *et al.*, 2004). The mutant was expressed in HEK293 cells along with WT DDR1 and stimulated with collagen. As shown in Figure 6D (phosphotyrosine [PY]), WT DDR1 was effectively phosphorylated upon collagen stimulation, whereas almost negligible phosphorylation of R105A was detected. We confirmed cell surface expression of R105A by cell surface immunostaining (Supplemental Figure S4C). Under these conditions, collagen-induced shedding of the R105A was reduced by 75% in comparison to WT (Figure 6D, top). We also examined mutants lacking the collagen-binding DD (ΔDD) or lacking both the DD and DLD (ΔDDΔDLD; Figure 6A) and found that neither the ΔDD nor the ΔDDΔDLD mutant was shed upon collagen stimulation (Figure 6E). Cell surface expression of those mutants was confirmed by cell surface immunostaining (Supplemental Figure S4D). From these results, we concluded that shedding of DDR1 requires collagen binding to the DD of DDR1 but is independent of DDR1 signaling.

Identification of DDR1 cleavage site and generation of shedding-resistant DDR1 mutants

To identify the ADAM10 cleavage site in DDR1, we established HEK293 cells stably expressing full-length DDR1 or DDR1ΔC, both of which have a FLAG tag at the C-terminus (Figure 7A). After collagen stimulation for 24 h, the remaining CTF of DDR1 was purified from cell lysates by anti-FLAG affinity chromatography, and the cleavage site(s) were analyzed by N-terminal sequencing. The data indicated that both DDR1-WT and DDR1ΔC were cleaved at the Pro-407–Val-408 bond located in the extracellular juxtamembrane region.

To elucidate the biological significance of DDR1 shedding, we next attempted to generate cleavage-resistant DDR1 mutants. We initially constructed various deletion mutants, but all the mutants were effectively shed upon collagen stimulation (Supplemental Figure S5). When the different cleavage sites identified in the deletion mutants were aligned, it was found that these cleavage sites were all located seven to nine amino acids upstream of the transmembrane domain (Supplemental Table S1). This suggests that ADAM10 prefers to cleave at a certain distance from the transmembrane domain, regardless of amino acid sequences.

According to the substrate specificity of ADAM10 analyzed by peptides (Caescu *et al.*, 2009), ADAM10 does not prefer Asp at P3–P3′ positions, Glu at P1′–P3′ positions, and Ala at P1′ position. Therefore we generated EAE and DAD mutants incorporating Asp or Glu substitutions at P1′ and P3′ positions of the DDR1 cleavage site (Figure 7A). Three additional mutants, DDAD, DDD, and 6xD, were also created, changing residues in P1, P1′, and P3′ in P1′–P3′ or in P3–P3′ to Asp, respectively. We also generated a 7xA mutant in which P3–P3′ were substituted with Ala (Figure 7A). These six mutants were expressed in HEK293 cells at a similar level to DDR1-WT, and cells were stimulated with collagen (Figure 7B). Collagen-induced shedding was reduced in EAE, DAD, DDAD, DDD, and 6xD mutations by 34, 46, 12, 38, and 57%, respectively (Figure 7B, table). All mutants showed phosphorylation in response to collagen (Figure 7B, PY), suggesting that they are all expressed on the cell surface and maintained collagen-binding property. We further analyzed the cleavage sites of these mutants. As shown by arrows in Figure 7C, DAD and 7xA were cleaved at Pro-407–Asp-408 or Ala-407–Ala-408, nine amino acids upstream of the transmembrane domain. DAD showed a second cleavage site at Pro-402–Arg-403. 6xD was cleaved at Ser-397–Leu-398 and/or Glu-399–Leu-400 located

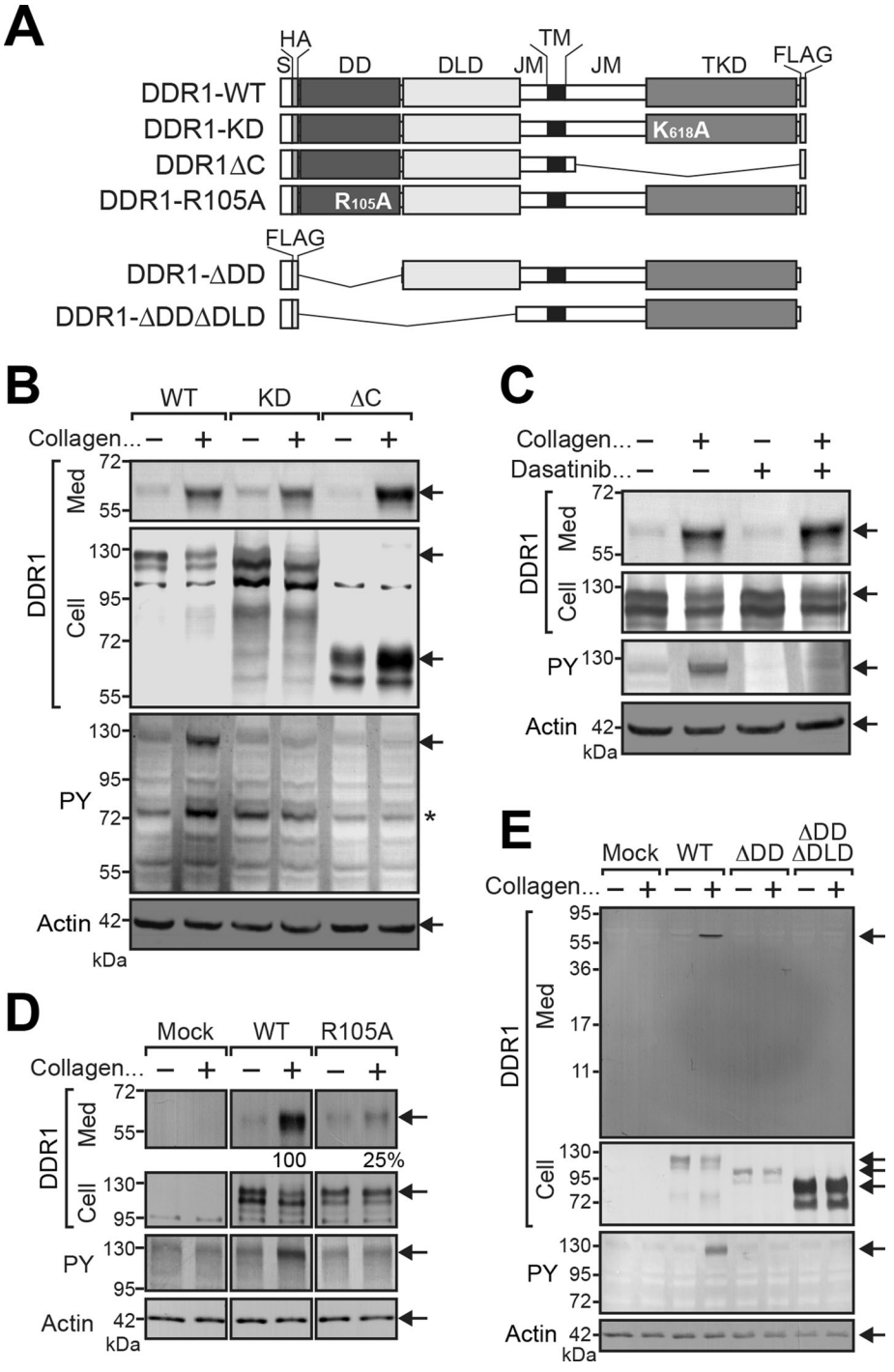

FIGURE 6: Collagen binding, but not DDR1 phosphorylation, is required for DDR1 shedding. (A) Schematic representation of mutant DDR1 constructs used in the experiments. DD, discoidin-homology domain; ΔC, cytoplasmic domain-deleted; DLD, discoidin-like domain; FLAG, FLAG tag (DYKDDDDK); HA, HA tag (YPYDVPDYA); JM, juxtamembrane region; KD, kinase dead; S, signal peptide; TM, transmembrane domain; TKD, tyrosine kinase domain. (B) HEK293 cells expressing DDR1-WT (WT), DDR1-KD (KD), or DDR1ΔC (ΔC) were treated with collagen I for 24 h. Conditioned media and cell lysates were analyzed by Western blotting using anti-DDR1 ectodomain (Med and Cell), anti–phosphotyrosine 4G10 (PY), or anti-actin. Asterisk indicates tyrosine-phosphorylated proteins other than DDR1. (C) HEK293 cells expressing DDR1-WT were treated with collagen I in the presence or absence of 50 nM dasatinib or vehicle control (DMSO) for 24 h. Conditioned media and cell lysates were analyzed by Western blotting using anti–DDR1 ectodomain (Med), antixDDR1 C-terminus (Cell), anti-PY, or anti-actin. (D) HEK293 cells were transiently transfected as indicated and treated with collagen for 24 h. Conditioned media and cell lysates were subjected to Western blotting using anti-DDR1 ectodomain and anti-actin antibodies. For the phosphotyrosine blot, cells treated with collagen for 1 h were used. The relative intensities of shed DDR1 are shown at the bottom of the top panel. (E) HEK293 cells were transfected with N-terminally FLAG-tagged DDR1 mutants as indicated and treated with collagen for 24 h. Conditioned media and cell lysates were analyzed by Western blotting as in D.

upstream of the initial cleavage site. We also confirmed that knockdown of ADAM10 inhibited shedding of those mutants, including 6xD (Figure 7E). These data show that the 6xD mutation is the most effective in abrogating collagen-induced ADAM10 cleavage in DDR1, forcing ADAM10 to cleave upstream sequences. We also introduced the 6xD mutation into DDR1ΔC (ΔC-6xD) and confirmed that the 6xD mutation reduced its shedding by 70% (Figure 7D). Both DDR1ΔC and ΔC-6xD were confirmed to be expressed on the cell surface in a similar manner by surface biotinylation assay (Supplemental Figure S4B). We confirmed that shedding of both DDR1ΔC and ΔC-6xD mutants was sensitive to ADAM10 knockdown (Figure 7E).

DDR1 shedding regulates the half-life of phosphorylation state of the receptor

Using the shedding-resistant 6xD mutant, we next addressed whether there are any correlations between the shedding of DDR1 ectodomain and the regulation of DDR1 phosphorylation. We established HEK293 cell lines stably expressing DDR1-WT or 6xD mutant. Both WT and 6xD were phosphorylated at 1 h after collagen stimulation (Figure 8, A, WT and PY, and B). We used a lower concentration of collagen (20 μg/ml) in this experiment, as adding 100 μg/ml of collagen resulted in formation of a thin collagen layer over the cells, causing cells to attach to the collagen layer rather than the bottom of plastic wells (unpublished data). Because this experiment involved washing out excess collagen, this was not ideal. We found that 20 μg/ml collagen was enough to cause DDR1 phosphorylation, and washing the cells did not detach them from the dish. The level of collagen-induced phosphorylation of DDR1-WT peaked at 1 h and then decreased upon washing out of collagen from the medium, with a half-life of ~1.5 h (Figure 8, A, WT and PY, and B). The level of DDR1-WT in cell lysates also decreased over the incubation time (Figure 8A, WT, Cell), which inversely correlated with the accumulation of shed DDR1 in the medium (Figure 8, A, WT and Med, and C). In contrast, phosphorylation of DDR1-6xD was sustained much

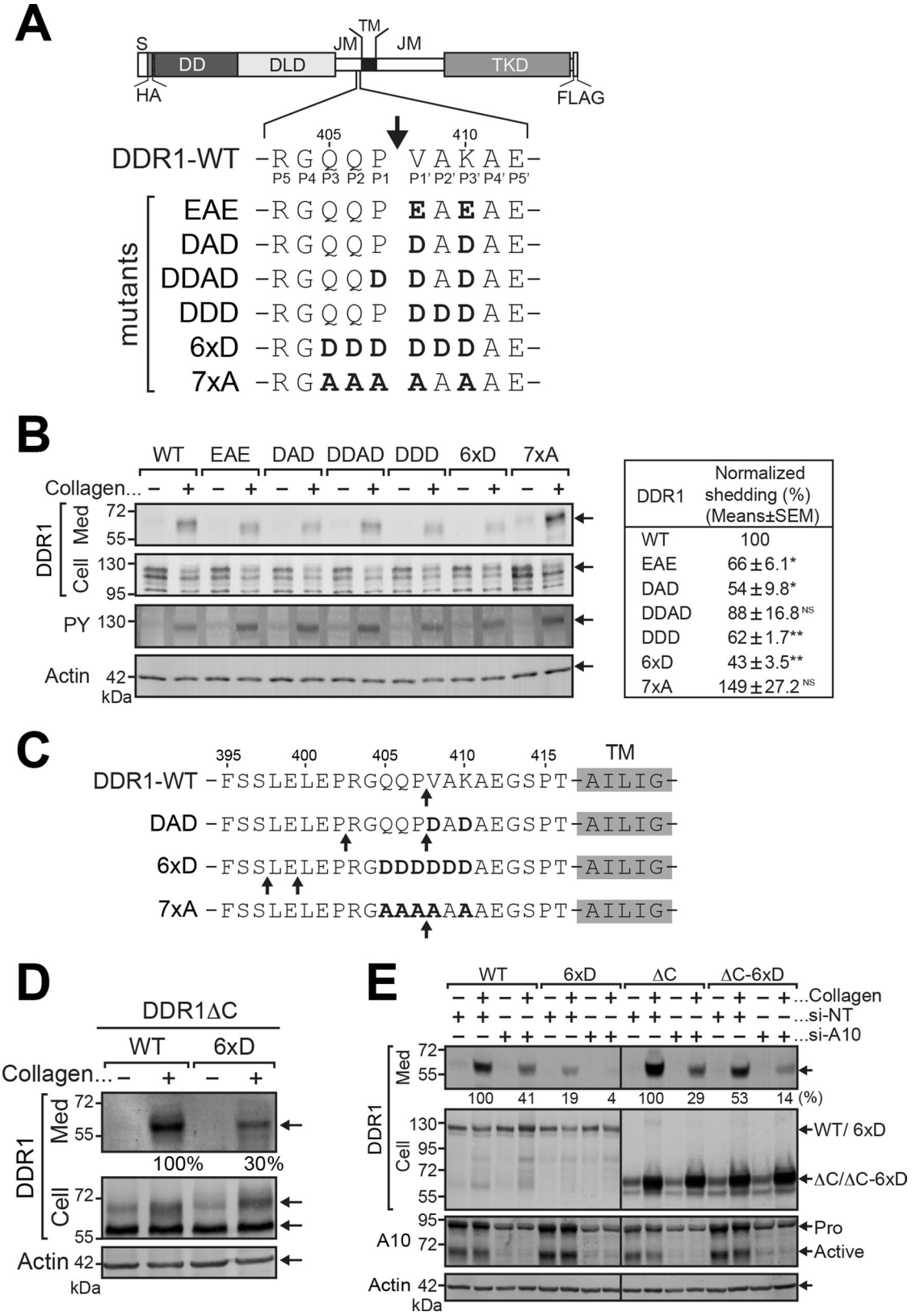

FIGURE 7: Engineering shedding-resistant DDR1 mutants. (A) Schematic representation of mutant DDR1 constructs used in the experiments. Arrow indicates the cleavage site identified. DD, discoidin-homology domain; DLD, discoidin-like domain; JM, juxtamembrane region; S, signal peptide; TKD, tyrosine kinase domain; TM, transmembrane domain. (B) HEK293 cells were transfected with expression plasmids for DDR1 mutants as indicated. Cells were treated with collagen for 24 h (DDR1 and Actin) or 1 h (PY). Conditioned media and cell lysates were subjected to Western blotting using anti-DDR1 (DDR1), anti-actin, and anti-PY antibodies. The band intensity of shed DDR1 was analyzed with Phoretix software, and fold changes were normalized to actin and DDR1 in cell lysates and sample volumes. The normalized

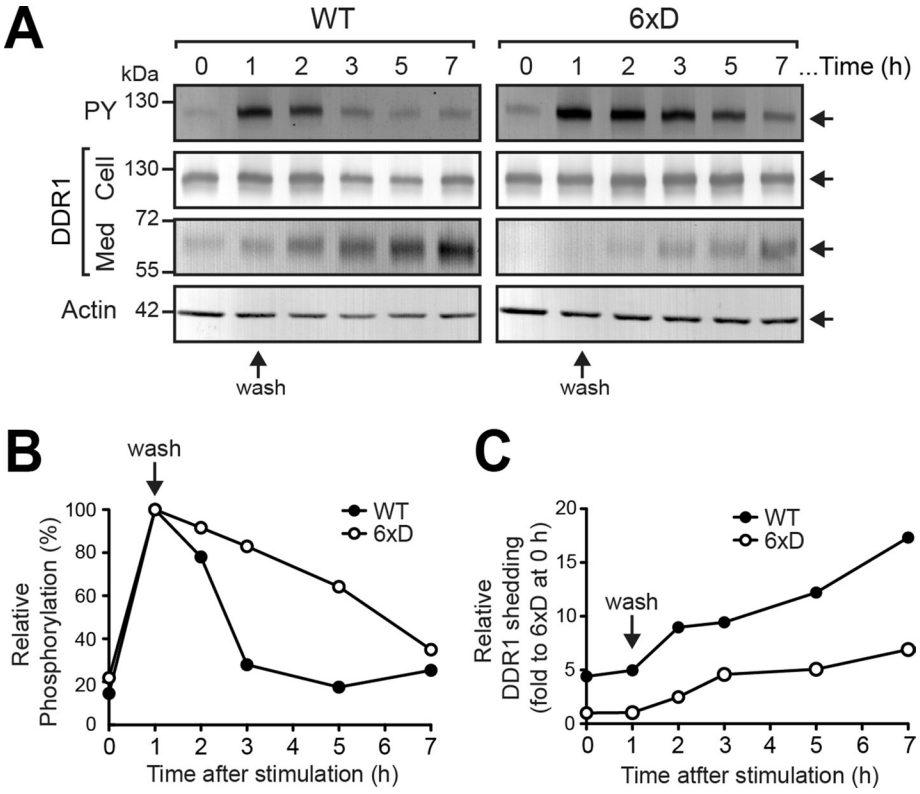

FIGURE 8: Reduced DDR1 shedding is associated with its sustained phosphorylation. (A) HEK293 stably expressing FLAG-tagged wild type (WT) or -6xD mutant DDR1 (6xD) were treated with collagen (20 μg/ml) for 1 h, excess collagen was then washed out, and cells were incubated further as indicated. RIPA lysates were collected at the indicated times and immunoprecipitated with anti-FLAG beads, followed by Western blotting with anti-DDR1 (Cell) and anti-PY antibodies. Shed DDR1 at each time point was analyzed by anti-DDR1 antibody (Med). Representative data from two independent experiments. (B) Relative intensities of phosphorylated DDR1 bands from A (PY). The intensities were standardized by the intensity of phosphorylated DDR1 in 1-h collagen-treated sample for each construct. (C) Relative band intensities of shed DDR1 in A (DDR1, Med). Relative intensities were normalized to the band intensity of shed DDR1-6xD at 0-h incubation time.

longer than WT, with a half-life of ~5 h (Figure 8, A, 6xD and PY, and B). This was accompanied by noticeably lower shedding of the DDR1 ectodomain (Figure 8, A, 6xD and Med, and C). These data suggest that ectodomain shedding of DDR1 is an important process to down-regulate its phosphorylation state of the receptor.

Role of DDR1 shedding on A431 cell migration on collagen matrix

During cell migration, cell adhesion and detachment of the cells from the matrix have to be coordinated with each other. It has been shown that DDR1 can facilitate cell adhesion to collagen matrices (Xu *et al.*, 2012), whereas DDR1 ectodomain shedding would disengage cell–collagen interaction through DDR1. We therefore investigated whether shedding of DDR1 has any role in cell migration on a collagen matrix. First, ADAM10 and/or DDR1 were knocked down in A431 cells and cells subjected to a wound-healing assay on a collagen matrix. We confirmed that ADAM10 and DDR1 proteins were effectively down-regulated by siRNA (Figure 9C). As shown in Figure 9, A and B, knockdown of ADAM10 significantly reduced wound closure by 45%, suggesting that ADAM10-dependent DDR1 shedding may play a role in cell migration. Of interest, DDR1 knockdown also resulted in a similar reduction of wound closure. This suggests that DDR1 positively promotes cell migration. Cells silenced for both ADAM10 and DDR1 did not show any additional effect on cell migration (Figure 9, A and B), suggesting that decreased cell migration by ADAM10 knockdown depended on the presence of DDR1. When cells transfected with si-NT were incubated with Mst, wound closure was also inhibited to similar levels (Figure 9, A and B).

To understand further the roles of ADAM10-dependent DDR1 shedding and DDR1-dependent collagen signaling in cell migration, we investigated the effect of overexpression of exogenous DDR1 or its mutants on migration of A431 cells on a collagen matrix. A431 cells stably expressing DDR1 WT, 6xD, ΔC, and ΔC-6xD were established (Figure 9F) and subjected to wound-closure assays. As shown in Figure 9, D and E, overexpression of DDR1-WT resulted in enhanced cell migration by 28% compared with mock cells, suggesting that ectopically expressed DDR1 further enhanced cell migration. In contrast, cells expressing 6xD migrated less than mock cells (13%) or cells expressing WT (32%; Figure 9, D and E), suggesting that inefficient shedding reduces DDR1-induced cell migration. Expression of DDR1ΔC did not affect cell migration on the collagen matrix (Figure 9, D and E), which is most likely due to lack of collagen signaling through DDR1ΔC (Figure 6B). On the other hand, migration of cells expressing ΔC-6xD, which do not transmit signals and shed 70%

shedding was calculated as described in *Materials and Methods*. Data are shown at the right and represent the means (%) ± SEM. $n = 3$ for each condition. *$p < 0.01$; **$p < 0.0001$; NS, not significant ($p > 0.05$; two-tailed Student's t test) compared with WT, collagen treated. Statistical analyses were performed with Prism, version 6 (GraphPad, La Jolla, CA). (C) Cleavage sites of DDR1 mutants were determined by N-terminal sequencing. Arrows indicate the identified cleavage sites. (D) HEK293 cells were transfected as indicated. Cells were treated with collagen for 24 h and analyzed as in B. The relative intensities of DDR1 shed forms are shown in the bottom of the top panel. (E) HEK293 cells stably expressing DDR1 mutants as indicated were transfected with siRNAs for ADAM10 (si-A10) or with nontargeting siRNA (si-NT). After 48 h, cells were treated with collagen I (100 μg/ml) for a further 24 h. Conditioned media and cell lysates were analyzed by Western blotting with antixDDR1 ectodomain (DDR1), anti-ADAM10 (A10), or anti-actin antibodies. The band intensity of shed DDR1 mutants was analyzed with Phoretix, and relative intensities were standardized to WT or ΔC treated with collagen. Data are shown at the bottom of the top panel. Active, active form of ADAM10; Pro, proform of ADAM10.

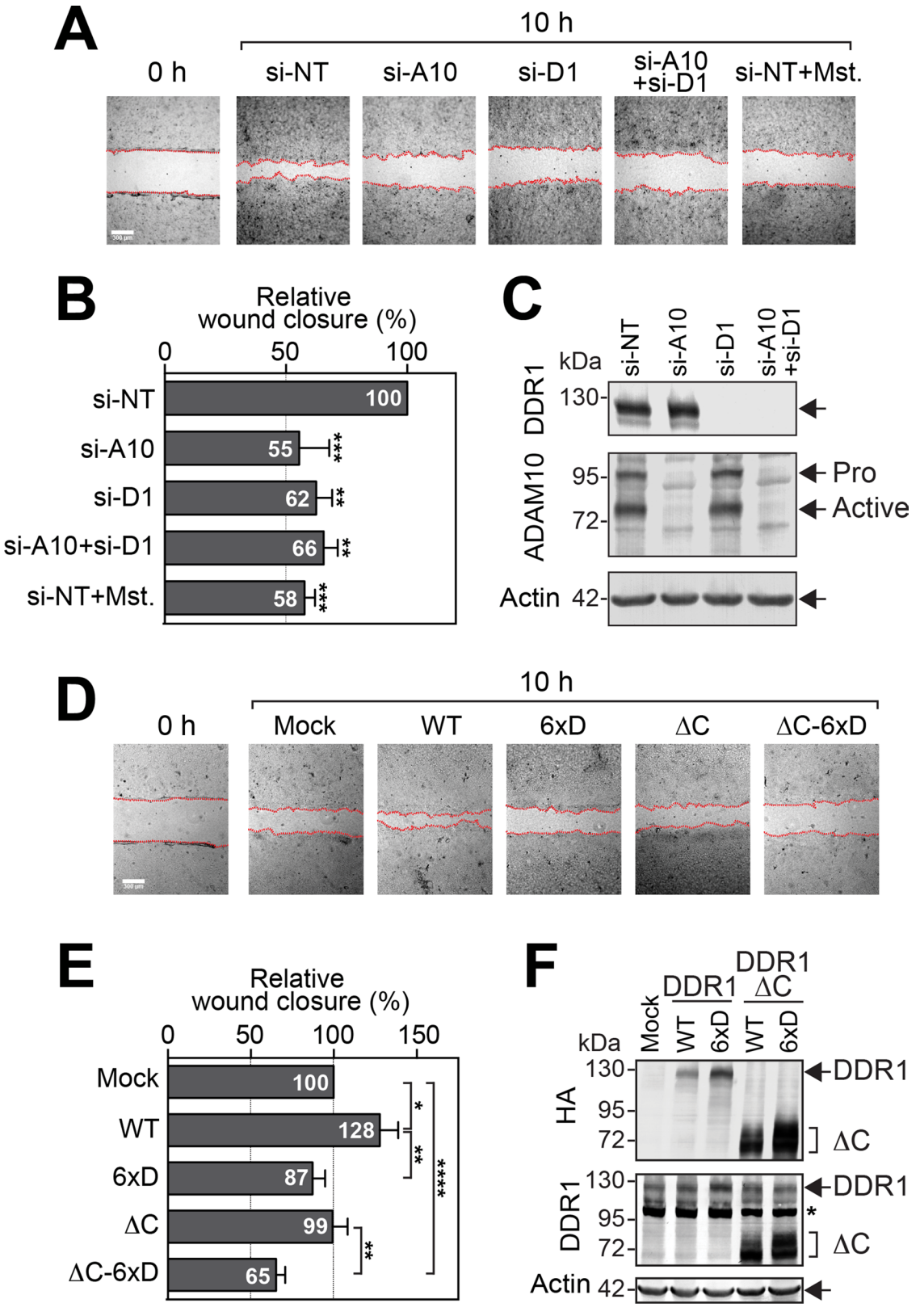

FIGURE 9: DDR1 ectodomain shedding is required for efficient cell migration on a collagen matrix. (A) A431 cells transfected with siRNAs for DDR1 (si-D1), ADAM10 (si-A10), or both DDR1 and ADAM10 (si-A10+si-D1) were subjected to wound-closure assay on a collagen matrix. Control cells were also treated with 50 μM Mst to inhibit DDR1 shedding. si-NT, nontargeting siRNA. Scale bar, 300 μm. Wound-healing edges of cells were traced and indicated with dashed lines. (B) Relative cell migration of each treatment in A. The data are presented as mean ± SEM ($n = 6$). **$p < 0.01$; ***$p < 0.005$ (one-way ANOVA) compared with each si-NT. $p < 0.05$ is considered statistically significant. Statistical analyses were performed with Prism, version 6 (GraphPad). (C) Knockdown levels of each protein were confirmed by

less efficiently than ΔC (Figure 7D), was significantly lower than that of mock (35%) or ΔC-expressing cells (34%). Taken together, these data suggest that DDR1 signaling and ADAM10-dependent DDR1 shedding independently contribute to efficient epithelial cell migration on collagen matrix.

DISCUSSION

DDR1 is widely expressed in epithelial cells of different tissues, including the skin, lung, liver, kidney, gut, colon, and brain (Barker *et al.*, 1995). DDR1-null mice have a severe phenotype: they are dwarfed and infertile and show abnormalities in epithelial organs, including mammary glands (Vogel *et al.*, 2001). It has also been reported that DDR1-knockout mice exhibit a high incidence of osteoarthritis in the temporomandibular joint (Schminke *et al.*, 2013). However, at the molecular level, it is not clear why lack of DDR1 results in these phenotypes. It has also not been clear whether DDR1 constitutively transmits signals to epithelial cells or whether the signaling is regulated in a spatiotemporal manner like that of other RTKs. In this study, we identified ADAM10 as the sheddase responsible for collagen-induced DDR1 ectodomain shedding and provided evidence that this ectodomain shedding is a regulatory mechanism that controls collagen signaling and cell migration.

In the absence of collagen stimulation, DDR1 is in a complex with ADAM10 (Figures 4 and 5). This interaction involves the ancillary domains of ADAM10 rather than the catalytic domain (Figure 4B). However, the orientation of the molecular complex does not allow ADAM10 to shed the DDR1 ectodomain. This interaction also likely causes steric hindrance that prevents TIMP-3 from binding to ADAM10. On collagen binding to the DD of DDR1, a reorientation would likely occur in the DDR1 ectodomain, which ultimately results in phosphorylation of the cytoplasmic domain of the receptor. At the same time, the reorientation of ectodomain would also render the cleavage site of DDR1 available for ADAM10, which initiates ectodomain shedding. It is possible that all DDR1 molecules on the cell surface are in complex with ADAM10 and ADAM10 in the complex is responsible for shedding DDR1 upon collagen stimulation. This idea is supported by our observation that collagen stimulation of A431 cells resulted in loss of endogenous ADAM10–DDR1 complex on the cell surface (Figure 5B). In addition, ectopic expression of ADAM10 in A431 cells did not induce the shedding, nor did it influence collagen-induced shedding (Figure 3D). Thus DDR1 shedding by ADAM10 is different from normal enzyme reactions, which are driven by turning over of substrate–enzyme interactions for catalysis. Recently it was reported that systemic overexpression of ADAM17 alone in mice did not result in increased levels of tumor necrosis factor-α (TNFα) unless lipopolysaccharide (LPS) was administered (Yoda *et al.*, 2013). Of interest, these authors did not find any differences in the level of TNFα release upon LPS administration between the controls and mice overexpressing TNF-α–converting enzyme. Their finding is similar to ours, and it is possible that ADAM17-dependent ectodomain shedding also may not be a simple enzyme–substrate interaction but involve specific complex formation with its substrate before shedding takes place.

It was recently reported that overexpression of MT1-MMP induced constitutive shedding of DDR1 in COS1 cells and T47D breast cancer cells (Fu *et al.*, 2013). However, our data indicated that endogenous MT1-MMP does not play a role in constitutive and collagen-induced shedding of DDR1 in A431 cells (Figure 3B). Fu *et al.* (2013) also indicated that they could not confirm endogenous MT1-MMP in HCC1806 cells to be a DDR1 sheddase. The role of MT1-MMP as DDR1 sheddase may thus be dependent on experimental conditions.

Our data showed that DDR1 shedding controls the half-life of the phosphorylation status of DDR1 upon collagen stimulation, and inefficient shedding caused prolonged phosphorylation status (Figure 8). Because collagen is a part of the solid extracellular matrix, its binding may prevent DDR1 from endocytosis, and shedding of DDR1 ectodomain allows remaining CTF to be endocytosed to terminate the signaling. On the other hand, inefficient shedding would retain phosphorylated DDR1 at the plasma membrane, resulting in a longer half-life of its phosphorylation status and persistent collagen signaling. Therefore ADAM10-mediated ectodomain shedding may be a major means to down-regulate DDR1-mediated collagen signaling. Our data suggest the possibility that all DDR1 molecules on the cell surface are in complex with ADAM10, and ADAM10 in the complex cannot be readily inhibited by TIMPs. It is possible that this TIMP-3 insensitivity is important for effective down-regulation of collagen signaling even in the presence of TIMPs.

Our data indicate that DDR1 signaling promotes cell migration on the collagen matrix, as knockdown of DDR1 reduces cell migration, and overexpression of DDR1 enhances cell migration, whereas the signaling defect DDR1 (ΔC) did not promote cell migration (Figure 9). It was shown that DDR1 and DDR2 activation enhances integrin-mediated cell adhesion (Xu *et al.*, 2012), and this may be a mechanism of DDR1-dependent cellular migration. We showed that shedding of the DDR1 ectodomain by ADAM10 is necessary for efficient cell migration on collagen, as ADAM10 knockdown inhibits cell migration (Figure 9, A–C). During cell migration, cell adhesion is essential, but detachment from the substratum is equally important. If cells fail to detach, they cannot migrate. In contrast to integrin-dependent cell adhesion, which can be regulated by inside-out signaling (Ridley *et al.*, 2003), dissociation of DDR1-dependent cell adhesion from collagen matrix cannot be controlled intracellularly, and it is likely that ectodomain shedding is the major mechanism to dissociate DDR1 from the collagen matrix. Inefficient shedding of DDR1 thus resulted in inhibition of cell migration on collagen matrix (Figure 9). It is unlikely that the shedding event itself promotes migration, as DDR1ΔC expression had no effect despite efficient shedding (Figure 9, D and E). Because efficient integrin-dependent adhesion needs DDR1 signaling (Xu *et al.*, 2012), it is possible that DDR1 shedding is coordinated with integrin-dependent cell adhesion. Similar proteolytic disengagement of cell adhesion has been demonstrated for CD44. CD44 is a hyaluronic acid receptor that promotes cell migration (Naor *et al.*, 2002). CD44 is shed by MT1-MMP, ADAM10, and ADAM17 (Kajita *et al.*, 2001; Murai *et al.*, 2004; Nagano *et al.*, 2004; Nakamura *et al.*, 2004), and the shedding by different metalloproteinases was shown to

Western blotting with anti-DDR1, anti-ADAM10, and anti-actin antibodies. Pro, proform of ADAMs; Active, active form of ADAMs. (D) A431 cells stably expressing DDR1-wild type (WT), -6xD, ΔC, and ΔC-6xD were subjected to wound-closure assay on a collagen matrix. Representative images from each treatment. Wound-healing edges of cells were traced and are indicated with dashed lines. (E) Data from D were analyzed as in B ($n = 16$). *$p < 0.05$; **$p < 0.01$; ****$p < 0.0001$ (two-tailed Student's *t* test). (F) A431 cells stably expressing DDR1 mutants were subjected to Western blotting to confirm the expression levels of each mutant. All constructs contain an N-terminal HA tag and a C-terminal FLAG tag. Asterisk indicates nonspecific band.

enhance cellular migration on hyaluronic acid–containing matrices (Kajita *et al.*, 2001; Murai *et al.*, 2004; Nagano *et al.*, 2004; Nakamura *et al.*, 2004). Thus ectodomain shedding of those ECM receptors is an important mechanism to regulate cell attachment and cell migration in different matrices.

ADAM10 is involved in shedding of various molecules, including epidermal growth factor, amyloid precursor protein, c-Met, Delta like ligand-1, E-cadherin, N-cadherin, VE-cadherin, ephrin A2 and A5, Fas-ligand, interleukin-6 receptor, klotho, Notch-1, CD44, and many others (Reiss and Saftig, 2009; Weber and Saftig, 2012). Although the sequence specificities and cleavage sites of ADAM10 have been analyzed using peptide libraries (Caescu *et al.*, 2009), ADAM10 still cleaves several unrelated substrates in a sequence-independent manner at a cellular level. ADAM10 and 17 cleave their type I transmembrane substrate proteins at 7–15 residues from the plasma membrane (Supplemental Table S1; Caescu *et al.*, 2009). We found that the distance from the transmembrane domain is the primary determinant for ectodomain shedding of DDR1, since deletion and substitution mutants of DDR1 were all cleaved at seven to nine amino acids upstream of the plasma membrane. The fact that ADAM10 has relaxed cleavage specificity may explain why ADAM10 can shed so many different membrane proteins, and this is likely to be an important feature of sheddases.

In conclusion, we have discovered a novel regulatory mechanism of a microenvironment signaling and cell migration through ADAM10-dependent DDR1 shedding in epithelial cells. Further investigation of collagen signaling through DDR1 would contribute to understanding how epithelial cells respond to signaling from their microenvironment and provide insight into complex epithelial biology.

MATERIALS AND METHODS

Cell culture and transfection

HEK293, HEK293-EBNA, A431, and MCF-7 cells were cultured in DMEM (Lonza, Verviers, Belgium) supplemented with 5% fetal bovine serum (FBS; GIBCO, Paisley, United Kingdom) and penicillin/streptomycin (PAA, Pasching, Austria) at 37°C, 5% CO_2. Cells were transiently transfected with expression plasmids using TransIT-2020 (Mirus, Madison, WI) according to the manufacturer's instructions.

Construction of DDR1 and ADAM10

The plasmids encoding DDR1 or ADAM10 mutants were based on the expression vector pSG5 and pCEP4 (Life Technologies, Paisley, United Kingdom). cDNA encoding human DDR1a (GenBank Accession Number NM_001954) was amplified by PCR using a cDNA library from HT1080 cells as a template, the forward primer containing the *Kpn*I site, 5′-GTC GGT ACC AGG AGC TAT GGG ACC AGA G-3′, and the reverse primer containing the *Bam*HI site, 5′-GGT GGA TCC TCA CAC CGT GTT GAG TGC AT-3′. The PCR product was cloned into pJET1.2/blunt cloning vector (Fermentas, Thermo Fisher Scientific, Rockford, IL) and the DNA sequence confirmed. The insert was then subcloned into pSG5 expression vector using *Kpn*I and *Bam*HI.

N-terminal FLAG (DYKDDDDK)-tagged DDR1 (DDR1-NF) and N-terminal hemagglutinin (HA; YPYDVPDYA)-C-terminal FLAG-tagged DDR1 (DDR1-NHA-CF) were constructed by the overlap extension PCR method (Ho *et al.*, 1989). N-terminal FLAG or HA epitopes were inserted three amino acids downstream of the signal peptide cleavage site (between Lys-23 and Gly-24), and the C-terminal FLAG epitope was introduced before the stop codon. All deletion and substitution DDR1 mutants were constructed by overlap extension PCR from full-length DDR1a clones, and all inserts were placed between *Kpn*I and *BamH*I sites of pSG5 or pCEP4 vectors. The DDR1 cytoplasmic deletion mutant (DDR1ΔC) was generated by the deletion of Glu-458–Val-876 in DDR1a. The discoidin homology domain deletion (ΔDD) and the DD and discoidin-like domain deletion (ΔDDΔDLD) mutants were made by the deletion of Cys-31—Cys-185 and Cys-31—Asp-367, respectively. The expected size of the ectodomain of ΔDD and ΔDDΔDLD is ~40 and 6 kDa, respectively. Kinase-dead DDR1 mutant (DDR1-KD) and collagen-binding-defective DDR1 mutant R105A were generated by introducing alanines at Lys-618 and at Arg-105, respectively.

cDNA encoding human ADAM10 (GenBank Accession Number NM_001110) was amplified as described, using the forward primer containing the *Bgl*II site, 5′-GAT AGA TCT CAG CGG AAG ATG GTG TTG C-3′, and the reverse primer containing the *Bgl*II site, 5′-GAT AGA TCT TGC AGT TAG CGT CTC ATG TG-3′. All ADAM10 mutants were constructed as described. The metalloproteinase deletion mutant (ADAM10ΔMP) was generated by the deletion of Thr-214—Ser-455 in ADAM10. An N-terminal FLAG tag was inserted immediately C-terminal to the protein convertase-recognition sequence RKKR. All of the amino acid numberings in this article are based on the full-length DDR1a or the full-length ADAM10, including their signal peptides.

Antibodies and reagents

The following antibodies were used: anti-DDR1 (C-20; sc-532; Santa Cruz Biotechnology, Dallas, TX), DDR1 extracellular domain antibody (AF2396; R&D Systems, Minneapolis, MN); anti-actin (I-19; sc-1616, Santa Cruz Biotechnology); anti-PY, clone 4G10 (Millipore, Watford, United Kingdom); anti-ADAM10 (ab1997; Abcam, Cambridge, United Kingdom); anti-ADAM10 ectodomain (AB936; R&D Systems); anti-ADAM17 (ab2051; Abcam); anti-MMP14 (clone EP1264Y; ab51074, Abcam); mouse monoclonal anti-MT1-MMP (222-1D8; Daiichi Fine Chemical Co., Takaoka, Japan); anti-TIMP-3 (136-13H4; IM43, Millipore); and anti-FLAG M2 antibody (Sigma-Aldrich, Dorset, United Kingdom). Secondary antibodies were purchased from the following sources: anti-mouse and anti-goat alkaline phosphatase–linked secondary antibodies from Sigma-Aldrich; anti-rabbit and anti-rat alkaline phosphatase–linked secondary antibodies from Promega (Southampton, United Kingdom); Alexa 568–conjugated anti-mouse immunoglobulin was purchased from Life Technologies. The broad-spectrum metalloproteinase inhibitor GM6001 was from Elastin Products Company (Owensville, MO), and Mst was from Tocris Bioscience (Bristol, United Kingdom). E-64, pepstatin A, AEBSF, and proteinase inhibitor (PI) cocktail III, PMA, IM, and dimethyl sulfoxide (DMSO) were from Sigma-Aldrich. γ-Secretase inhibitor X (L-685, 458) was obtained from Calbiochem (Darmstadt, Germany). Dasatinib was purchased from LC Laboratories (Woburn, MA).

DDR1 stimulation and detection of shed DDR1 in media

HEK293 cells in 12-well plates were transfected with DDR1 expression vectors using TransIT-2020. The next day, the medium was removed, and cells were incubated in 500 µl of serum-free medium with or without PureCol (bovine collagen type I; Advanced BioMatrix, San Diego, CA) at a concentration of 100 µg/ml for 24 h. After stimulation, the media were collected and centrifuged to remove cell debris, and then proteins were precipitated with trichloroacetic acid (TCA) and dissolved in 1× SDS-loading buffer (21 mM 2-amino-2-methyl-1,3,-propanediol, 15.5 mM HCl, 100 mM Tris-HCl, pH 8.0, 75 mM NaCl, 1% SDS, 20% glycerol, 5% 2-mercaptethanol). Cells were lysed in 80 µl of 1× SDS-loading buffer, and the lysates were heated at 95°C for 25 min. Samples were analyzed by SDS–PAGE and Western blotting. To detect DDR1 phosphorylation, cells were cultured in serum-free medium containing 100 µg/ml PureCol

collagen for 1 h and lysed with 1× SDS-loading buffer containing 2 mM Na_3VO_4. To analyze the effect of phorbol ester and calcium ionophore on DDR1 shedding, cells were treated with 25 ng/ml PMA, 1 µM IM, or 0.001% DMSO in serum-free medium for 1 h. Cells and media were collected as described.

Surface biotinylation and coimmunoprecipitation

For a tandem coimmunoprecipitation assay, cell surface biotinylation was carried out on A431 cells expressing DDR1-NF, DDR1ΔC-NF, or mock vector. Transfected A431 cells were washed three times with chilled phosphate-buffered saline (PBS) containing PI cocktail III (Sigma-Aldrich). Cells were then incubated with 2 mg/ml sulfo-NHS-biotin (Thermo Fisher Scientific) in the same buffer at 4°C for 30 min. The reaction was terminated by washing the cells three times with 25 mM lysine in PBS. The cells were lysed in the lysis buffer (1% Triton X-100, 50 mM Tris-HCl, pH 8.0, 150 mM NaCl, 0.02% NaN_3, 10 µM GM6001, and PI), and the lysate was sonicated on ice using an ultrasonic processor (Vibra-Cell, VCX130; Sonics and Materials, Suffolk, United Kingdom) at amplitude of 40% for eight cycles of 15-s sonication and 5-s pause. The sonicated samples were centrifuged at 16,000 × *g* for 15 min at 4°C, and the supernatants were incubated with anti-FLAG M2 magnetic beads (Sigma-Aldrich) at 4°C overnight. Beads were washed three times with the lysis buffer and then three times with TBS (50 mM Tris-HCl, pH 8.0, 150 mM NaCl, 0.02% NaN_3) containing 10 µM GM6001 and PI. The protein complexes were eluted in 0.5 mg/ml 1× FLAG peptide (Cambridge Research Biochemicals, Cleveland, United Kingdom) in TBS. Next the eluates were diluted in the lysis buffer and incubated with streptavidin–agarose beads (GE Healthcare Little Chalfont, United Kingdom) at 4°C for 2 h. Beads were washed three times with the lysis buffer and then three times with TBS containing 10 µM GM6001 and PI. The biotinylated proteins were eluted with reducing 1× SDS-loading buffer. To detect endogenous DDR1/ADAM10 interaction in A431 cells, a tandem coimmunoprecipitation assay was also performed. Cell lysates were prepared as described and then incubated with anti-DDR1 ectodomain antibody bound to Dynabeads Protein G (Invitrogen) at 4°C overnight. The bound materials were eluted with TBS containing 6 M urea, 10 µM Mst, and PI. The eluate was subjected to streptavidin affinity precipitation as described.

For a standard coimmunoprecipitation assay, cells were lysed in Triton-lysis buffer, and lysates were incubated with anti-FLAG M2 magnetic beads at 4°C overnight. Beads were washed, and the protein complexes were eluted as described. The eluates were mixed with 2× SDS-loading buffer and analyzed by Western blotting.

Establishment of DDR1 mutant–expressing cell lines

Recombinant DDR1 constructs were cloned into pCEP4 expression vector (Invitrogen, Life Technologies). HEK293-EBNA cells were transfected with the pCEP4 vectors using TransIT-2020, and transfectants were selected by treatment with 800 µg/ml hygromycin B (Sigma-Aldrich) over 3 wk. A431 cells were also used to generate stable cell lines and selected with 400 µg/ml hygromycin B. Transfected stable cell lines were maintained in DMEM containing 5% FBS, penicillin/streptomycin, and hygromycin B (400 µg/ml for A431, 800 µg/ml for HEK293) at 37°C, 5% CO_2.

Purification of CTF and N-terminal amino acid sequencing

HEK293 cells expressing C-terminally FLAG-tagged DDR1 mutants were cultured until 90–100% confluent in 15-cm dishes (8 dishes/mutant) and then stimulated with 100 µg/ml collagen I in serum-free DMEM for 24 h. Cells were harvested by centrifugation and lysed in 3 ml of 1% SDS, followed by addition of 27 ml of RIPA buffer (1% Triton X-100, 1% deoxycolic acid, 50 mM Tris-HCl, pH 8.0, 150 mM NaCl, 0.02% NaN_3, PI) and sonicated on ice using Vibra-Cell at amplitude 40% for eight cycles of 15-s sonication and 5-s pause. The sonicated samples were centrifuged at 16,000 × *g* for 15 min at 4°C and the supernatants collected (30 ml/mutant). To purify CTFs, the supernatants were incubated with 100 µl of anti-FLAG M2 magnetic beads at 4°C overnight with rotation. After washing of beads three times with RIPA buffer containing 0.1% SDS and twice with TBS, the bound proteins were eluted in 0.5 mg/ml FLAG peptide in TBS and analyzed by Western blotting using anti-FLAG antibody detecting CTFs of DDR1. A431 cells stably expressing C-terminally FLAG-tagged DDR1 were treated with 1 µM IM for 1 h, and generated CTFs were purified as described.

For N-terminal amino acid sequencing, the purified CTFs were subjected to SDS–PAGE and electrotransferred onto a polyvinylidene fluoride (PVDF) membrane in 3-[cyclohexylamino]-1-propanesulfonic acid/MtOH buffer (Matsudaira, 1987). The membrane was stained with 0.1% Coomassie brilliant blue R-250 and then destained in 50% methanol/10% acetic acid. After washing of the membrane with distilled water, the CTF bands were excised and sequenced by automated Edman degradation using a Procise 494HT amino acid sequencer (Applied Biosystems, Life Technologies) with on-line phenylthiohydantoin analysis.

SDS–PAGE and Western blotting

Total cell lysates were prepared by the addition of 1× SDS–PAGE loading buffer containing 2-mercaptethanol to cells in the culture plate and subsequent boiling for 25 min. To detect proteins in culture supernatant, the medium was treated with 10% TCA. Cell lysate, TCA-precipitated proteins, and immunoprecipitated materials were separated by SDS–PAGE as described (Bury, 1981), and proteins in the gel were transferred onto a PVDF membrane using a Trans-Blot Turbo Transfer System (Bio-Rad, Hemel Hempstead, United Kingdom). After blocking of the membrane with 10% skim milk in PBS, the membrane was probed with appropriate primary antibodies. Proteins were visualized using an alkaline phosphatase–conjugated secondary antibody. For analysis of the shed form of DDR1-ΔDD and DDR1-ΔDDΔDLD, 16% Tris-tricine gel was used. Band intensities were measured with Phoretix 1D software (Totallab, Newcastle upon Tyne, United Kingdom) in all experiments in this article. To analyze shedding of mutant DDR1s, normalized shedding was calculated using the equation

$$\text{Normalized collagen-induced shedding (\%)} = (BI_{\text{shed form}} \times VF)/[(BI_{\text{shed form}} \times VF) + (BI_{\text{remaining DDR1 in cell}} \times VF)] \times 100$$

where BI indicates band intensity and VF indicates volume factor, (total sample volume)/(sample volume applied in the lane). Data are shown in each figure as relative shedding against WT DDR1.

RNA interference and reverse transcriptase-PCR

The following ON-TARGETplus SMARTpool siRNAs (Thermo Fisher Scientific) were used: human DDR1 (hDDR1), hADAM8, hADAM9, hADAM10, hADAM17, hADAM19, hMMP14 (MT1-MMP), and nontargeting siRNA #4. Cells were seeded in 24-well plates (3.5×10^4 cells/well for A431, 2.5×10^4 cells/well for HEK293) together with 20 nM SMARTpool siRNA using 3 µl of INTERFERin (Polyplus-transfection, Illkirch, France) in a total reaction volume of 0.6 ml/well (reverse transfection protocol). At 48 h after transfection, cells were treated for a further 24 h with serum-free DMEM in the presence or absence of 100 µg/ml collagen I. Conditioned media were collected, and cells were lysed in SDS-loading buffer for Western blotting analysis. Total RNAs were isolated with

QIAamp RNA Blood Mini Kit (Qiagen, Hilden, Germany), and RNAs were used for reverse transcriptase (RT)-PCR analysis with SuperScript One-Step RT-PCR System (Invitrogen, Life Technologies) according to the manufacturer's instructions. The primer sequences used in RT-PCR were as follows: hADAM8 forward, 5′-CACAGAGGATGGCACTGCGTATGA-3′, and reverse, 5′-CGTGCACCTCAGTCAGCAGCTT-3′ (annealing temperature [Ta], 57°C); hADAM9 forward, 5′-GGGGCTATGTGGAGGGAGTT-3′, and reverse, 5′-CATACCGGGTCTGTGGCAAG-3′ (Ta, 50°C); hADAM10 forward, 5′-CAATTTGGGGGTGGGAGGTG-3′, and reverse, 5′-GCCTCCTAGCCTTGATTGGC-3′ (Ta, 50°C); fADAM17 forward, 5′-CAACTCCTGCAAGGTGTGCT-3′, and reverse, 5′ -AACCAGGACAGACCCAACGA-3′ (Ta, 50°C); hADAM19 forward, 5′-GAGGAGGAGGGTGACATGCT-3′, and reverse, 5′-CCACACTCTCAGGGGGCATA-3′ (Ta, 50°C); and hGAPDH forward, 5′-TTCACCACCATGGAGAAGGC-3′, and reverse, 5′-GGCATGGACTGTGGTCATGA-3′ (Ta, 50°C). Amplified products were electrophoresed in 3% agarose gels and visualized by ethidium bromide staining.

In situ PLA

In situ PLA was performed using Duolink II (Olink Bioscience, Uppsala, Sweden) as described previously (Woskowicz *et al.*, 2013). HEK293 stable cell lines or A431 cells were cultured on gelatin-coated cover glasses and fixed with 3% paraformaldehyde/PBS for 10 min at room temperature, followed by 30 min of incubation with blocking solution (Duolink II) at 37°C. After blocking, cells were immunostained with 20 µg/ml anti-DDR1 ectodomain goat antibody and 10 µg/ml anti-ADAM10 ectodomain mouse antibody for 2 h at room temperature, followed by 1 h of incubation at 37°C with a secondary antibody to goat immunoglobulin G (IgG) conjugated with PLA probe PLUS and a secondary antibody to mouse IgG conjugated with PLA probe MINUS. For detection of PLA signals, Duolink II detection reagents orange was used. The PLA signals were observed by wide-field TE2000-E microscope equipped with a Hamamatsu Orca ER charge-coupled camera (Hamamatsu, Hamamatsu, Japan) with a Nikon Plan Fluor 10× dry lens with numerical aperture (NA) 0.3 (Nikon, Melville, NY) and Volocity acquisition software (PerkinElmer-Cetus, Waltham, MA). The PLA signal is visible as a distinct fluorescent spot when both probes are in close proximity of <40 nm. The nucleus was counterstained with 4′,6-diamidino-2-phenylindole (DAPI). For washing steps, Duolink II Wash Buffer A and B (Olink Bioscience) were used.

DDR1 phosphorylation assay

For detection of DDR1 phosphorylation, cells were treated with 100 µg/ml collagen I (PureCol) for 1 h as described and lysed with 1× SDS-loading buffer containing 2 mM Na_3VO_4, followed by Western blotting using anti–phosphotyrosine 4G10 antibody.

To address correlation between shedding and phosphorylation of DDR1, HEK293 cell lines stably expressing C-terminally FLAG-tagged DDR1-wild-type or -6xD mutant were established, and immunoprecipitation assay was performed. In brief, cells were seeded in a 12-well multiwell plate and incubated at 37°C/5% CO_2 for 24 h. Cells were rinsed with serum-free DMEM and stimulated with or without 20 µg/ml collagen I (PureCol) for 1 h. Then cells were washed with serum-free medium and further incubated in serum-free medium up to 7 h in total. Cells were lysed in RIPA buffer containing 0.1% SDS, 2 mM Na_3VO_4, 10 µM GM6001, and PI at each incubation period (0, 1, 2, 3, 5, 7 h). Lysates were incubated with anti-FLAG M2 magnetic beads at 4°C overnight with rotation. Beads were washed three times with the lysis buffer and then three times with TBS containing 2 mM Na_3VO_4, 10 µM GM6001, and PI. The protein complexes were eluted in 500 µg/ml 1× FLAG peptide in TBS containing 2 mM Na_3VO_4. The eluates were mixed with 2× SDS-loading buffer and analyzed by Western blotting.

A431 cell migration using the ibidi Culture-Insert

For A431 cell migration assay, an ibidi Culture-Insert (ibidi, Martinsried, Germany) consisting of two reservoirs separated by a 500-µm-thick wall was used. PureCol (bovine type I, 3.1 mg/ml; Advanced BioMatrix) and Cellmatrix type I-A collagen (porcine, 3.0 mg/ml; Nitta Gelatin, Osaka, Japan) were mixed at 1:1 ratio in 1× RPMI medium and neutralized on ice. Twenty four-well plates were coated with the collagen mixture (450 µl/well) and allowed to form a collagen layer for 1 h at 37°C/5% CO_2. A Culture-Insert was placed into one well of the 24-well plate and slightly pressed on the top to ensure tight adhesion. A431 cells (6×10^5/ml) expressing DDR1 mutant were seeded into the two reservoirs of the same insert (80 µl/reservoir) and incubated overnight at 37°C/5% CO_2. The next day, the inserts were gently removed and washed once with DMEM medium. The wells were filled with complete growth media, and the cells were cultured for 10 h at 37°C/5% CO_2. Mst 50 µM in complete growth medium was used as a control. The images were captured at time points 0 and 10 h by a Nikon TE2000-E microscope equipped with a Hamamatsu Orca ER charge-coupled device camera using a Nikon Plan Fluor 4× dry lens with NA 0.13. The migration areas were measured by ImageJ (National Institutes of Health, Bethesda, MD) software, and the data are shown as mean (± SEM) percentage of migration area relative to cells transfected with mock vector.

ACKNOWLEDGMENTS

We are grateful to Hideaki Nagase and Linda Troeberg for critical reading of the manuscript. This work was supported by an Arthritis Research UK core grant to the Kennedy Institute of Rheumatology, Arthritis Research UK Programme Grant 19797, and Cancer Research UK Project Grant C1507/A12015.

REFERENCES

Abdulhussein R, McFadden C, Fuentes-Prior P, Vogel WF (2004). Exploring the collagen-binding site of the DDR1 tyrosine kinase receptor. J Biol Chem 279, 31462–31470.

Ahonen M, Poukkula M, Baker AH, Kashiwagi M, Nagase H, Eriksson JE, Kahari VM (2003). Tissue inhibitor of metalloproteinases-3 induces apoptosis in melanoma cells by stabilization of death receptors. Oncogene 22, 2121–2134.

Amour A, Knight CG, English WR, Webster A, Slocombe PM, Knauper V, Docherty AJ, Becherer JD, Blobel CP, Murphy G (2002). The enzymatic activity of ADAM8 and ADAM9 is not regulated by TIMPs. FEBS Lett 524, 154–158.

Amour A, Knight CG, Webster A, Slocombe PM, Stephens PE, Knauper V, Docherty AJ, Murphy G (2000). The in vitro activity of ADAM-10 is inhibited by TIMP-1 and TIMP-3. FEBS Lett 473, 275–279.

Barker KT, Martindale JE, Mitchell PJ, Kamalati T, Page MJ, Phippard DJ, Dale TC, Gusterson BA, Crompton MR (1995). Expression patterns of the novel receptor-like tyrosine kinase, DDR, in human breast tumours. Oncogene 10, 569–575.

Blobel CP (2005). ADAMs: key components in EGFR signalling and development. Nat Rev Mol Cell Biol 6, 32–43.

Bury AF (1981). Analysis of protein and peptide mixtures—evaluation of 3 sodium dodecyl sulfate-polyacrylamide gel-electrophoresis buffer systems. J Chromatogr 213, 491–500.

Caescu CI, Jeschke GR, Turk BE (2009). Active-site determinants of substrate recognition by the metalloproteinases TACE and ADAM10. Biochem J 424, 79–88.

Chan KM, Wong HL, Jin G, Liu B, Cao R, Cao Y, Lehti K, Tryggvason K, Zhou Z (2012). MT1-MMP inactivates ADAM9 to regulate FGFR2 signaling and calvarial osteogenesis. Dev Cell 22, 1176–1190.

Chesneau V, Becherer JD, Zheng Y, Erdjument-Bromage H, Tempst P, Blobel CP (2003). Catalytic properties of ADAM19. J Biol Chem 278, 22331–22340.

Day E, Waters B, Spiegel K, Alnadaf T, Manley PW, Buchdunger E, Walker C, Jarai G (2008). Inhibition of collagen-induced discoidin domain receptor 1 and 2 activation by imatinib, nilotinib and dasatinib. Eur J Pharmacol 599, 44–53.

Dreux AC, Lamb DJ, Modjtahedi H, Ferns GA (2006). The epidermal growth factor receptors and their family of ligands: their putative role in atherogenesis. Atherosclerosis 186, 38–53.

Fu HL, Sohail A, Valiathan RR, Wasinski BD, Kumarasiri M, Mahasenan KV, Bernardo MM, Tokmina-Roszyk D, Fields GB, Mobashery S, Fridman R (2013). Shedding of discoidin domain receptor 1 by membrane-type matrix metalloproteinases. J Biol Chem 288, 12114–12129.

Goh LK, Sorkin A (2013). Endocytosis of receptor tyrosine kinases. Cold Spring Harb Perspect Biol 5, a017459.

Ho SN, Hunt HD, Horton RM, Pullen JK, Pease LR (1989). Site-directed mutagenesis by overlap extension using the polymerase chain reaction [see comments]. Gene 77, 51–59.

Kajita M, Itoh Y, Chiba T, Mori H, Okada A, Kinoh H, Seiki M (2001). Membrane-type 1 matrix metalloproteinase cleaves CD44 and promotes cell migration. J Cell Biol 153, 893–904.

Labrador JP, Azcoitia V, Tuckermann J, Lin C, Olaso E, Manes S, Bruckner K, Goergen JL, Lemke G, Yancopoulos G, *et al.* (2001). The collagen receptor DDR2 regulates proliferation and its elimination leads to dwarfism. EMBO Rep 2, 446–452.

Le Gall SM, Bobe P, Reiss K, Horiuchi K, Niu XD, Lundell D, Gibb DR, Conrad D, Saftig P, Blobel CP (2009). ADAMs 10 and 17 represent differentially regulated components of a general shedding machinery for membrane proteins such as transforming growth factor alpha, L-selectin, and tumor necrosis factor alpha. Mol Biol Cell 20, 1785–1794.

Leitinger B (2003). Molecular analysis of collagen binding by the human discoidin domain receptors, DDR1 and DDR2. Identification of collagen binding sites in DDR2. J Biol Chem 278, 16761–16769.

Leitinger B (2011). Transmembrane collagen receptors. Annu Rev Cell Dev Biol 27, 265–290.

Leitinger B (2014). Discoidin domain receptor functions in physiological and pathological conditions. Int Rev Cell Mol Biol 310, 39–87.

Leitinger B, Hohenester E (2007). Mammalian collagen receptors. Matrix Biol 26, 146–155.

Lemmon MA, Schlessinger J (2010). Cell signaling by receptor tyrosine kinases. Cell 141, 1117–1134.

Lu KK, Trcka D, Bendeck MP (2011). Collagen stimulates discoidin domain receptor 1-mediated migration of smooth muscle cells through Src. Cardiovasc Pathol 20, 71–76.

Marmor MD, Yarden Y (2004). Role of protein ubiquitylation in regulating endocytosis of receptor tyrosine kinases. Oncogene 23, 2057–2070.

Matsudaira P (1987). Sequence from picomole quantities of proteins electroblotted onto polyvinylidene difluoride membranes. J Biol Chem 262, 10035–10038.

Murai T, Miyazaki Y, Nishinakamura H, Sugahara KN, Miyauchi T, Sako Y, Yanagida T, Miyasaka M (2004). Engagement of CD44 promotes Rac activation and CD44 cleavage during tumor cell migration. J Biol Chem 279, 4541–4550.

Nagano O, Murakami D, Hartmann D, De Strooper B, Saftig P, Iwatsubo T, Nakajima M, Shinohara M, Saya H (2004). Cell-matrix interaction via CD44 is independently regulated by different metalloproteinases activated in response to extracellular Ca(2+) influx and PKC activation. J Cell Biol 165, 893–902.

Nakamura H, Suenaga N, Taniwaki K, Matsuki H, Yonezawa K, Fujii M, Okada Y, Seiki M (2004). Constitutive and induced CD44 shedding by ADAM-like proteases and membrane-type 1 matrix metalloproteinase. Cancer Res 64, 876–882.

Naor D, Nedvetzki S, Golan I, Melnik L, Faitelson Y (2002). CD44 in cancer. Crit Rev Clin Lab Sci 39, 527–579.

Porter AC, Vaillancourt RR (1998). Tyrosine kinase receptor-activated signal transduction pathways which lead to oncogenesis. Oncogene 17, 1343–1352.

Reiss K, Saftig P (2009). The "a disintegrin and metalloprotease" (ADAM) family of sheddases: physiological and cellular functions. Semin Cell Dev Biol 20, 126–137.

Ridley AJ, Schwartz MA, Burridge K, Firtel RA, Ginsberg MH, Borisy G, Parsons JT, Horwitz AR (2003). Cell migration: integrating signals from front to back. Science 302, 1704–1709.

Schminke B, Muhammad H, Bode C, Sadowski B, Gerter R, Gersdorff N, Burgers R, Monsonego-Ornan E, Rosen V, Miosge N (2013). A discoidin domain receptor 1 knock-out mouse as a novel model for osteoarthritis of the temporomandibular joint. Cell Mol Life Sci 71, 1081–1096.

Scilabra SD, Troeberg L, Yamamoto K, Emonard H, Thogersen I, Enghild JJ, Strickland DK, Nagase H (2013). Differential regulation of extracellular tissue inhibitor of metalloproteinases-3 levels by cell membrane-bound and shed low density lipoprotein receptor-related protein 1. J Biol Chem 288, 332–342.

Shintani Y, Fukumoto Y, Chaika N, Svoboda R, Wheelock MJ, Johnson KR (2008). Collagen I-mediated up-regulation of N-cadherin requires cooperative signals from integrins and discoidin domain receptor 1. J Cell Biol 180, 1277–1289.

Shiomi T, Lemaitre V, D'Armiento J, Okada Y (2010). Matrix metalloproteinases, a disintegrin and metalloproteinases, and a disintegrin and metalloproteinases with thrombospondin motifs in non-neoplastic diseases. Pathol Int 60, 477–496.

Shrivastava A, Radziejewski C, Campbell E, Kovac L, McGlynn M, Ryan TE, Davis S, Goldfarb MP, Glass DJ, Lemke G, Yancopoulos GD (1997). An orphan receptor tyrosine kinase family whose members serve as nonintegrin collagen receptors. Mol Cell 1, 25–34.

Slack BE, Siniaia MS, Blusztajn JK (2006). Collagen type I selectively activates ectodomain shedding of the discoidin domain receptor 1: involvement of Src tyrosine kinase. J Cell Biochem 98, 672–684.

Sunnarborg SW, Hinkle CL, Stevenson M, Russell WE, Raska CS, Peschon JJ, Castner BJ, Gerhart MJ, Paxton RJ, Black RA, Lee DC (2002). Tumor necrosis factor-alpha converting enzyme. (TACE) regulates epidermal growth factor receptor ligand availability. J Biol Chem 277, 12838–12845.

Thorp E, Vaisar T, Subramanian M, Mautner L, Blobel C, Tabas I (2011). Shedding of the Mer tyrosine kinase receptor is mediated by ADAM17 protein through a pathway involving reactive oxygen species, protein kinase Cdelta, and p38 mitogen-activated protein kinase (MAPK). J Biol Chem 286, 33335–33344.

Valencia K, Ormazabal C, Zandueta C, Luis-Ravelo D, Anton I, Pajares MJ, Agorreta J, Montuenga LM, Martinez-Canarias S, Leitinger B, Lecanda F (2012). Inhibition of collagen receptor discoidin domain receptor-1 (DDR1) reduces cell survival, homing, and colonization in lung cancer bone metastasis. Clin Cancer Res 18, 969–980.

Vogel W (1999). Discoidin domain receptors: structural relations and functional implications. FASEB J 13(Suppl), S77–S82.

Vogel WF (2002). Ligand-induced shedding of discoidin domain receptor 1. FEBS Lett 514, 175–180.

Vogel WF, Abdulhussein R, Ford CE (2006). Sensing extracellular matrix: an update on discoidin domain receptor function. Cell Signal 18, 1108–1116.

Vogel WF, Aszodi A, Alves F, Pawson T (2001). Discoidin domain receptor 1 tyrosine kinase has an essential role in mammary gland development. Mol Cell Biol 21, 2906–2917.

Vogel W, Gish GD, Alves F, Pawson T (1997). The discoidin domain receptor tyrosine kinases are activated by collagen. Mol Cell 1, 13–23.

Weber S, Saftig P (2012). Ectodomain shedding and ADAMs in development. Development 139, 3693–3709.

Woskowicz AM, Weaver SA, Shitomi Y, Ito N, Itoh Y (2013). MT-LOOP-dependent localization of membrane type I matrix metalloproteinase (MT1-MMP) to the cell adhesion complexes promotes cancer cell invasion. J Biol Chem 288, 35126–35137.

Xu H, Bihan D, Chang F, Huang PH, Farndale RW, Leitinger B (2012). Discoidin domain receptors promote alpha1beta1- and alpha2beta1-integrin mediated cell adhesion to collagen by enhancing integrin activation. PLoS One 7, e52209.

Xu L, Peng H, Glasson S, Lee PL, Hu K, Ijiri K, Olsen BR, Goldring MB, Li Y (2007). Increased expression of the collagen receptor discoidin domain receptor 2 in articular cartilage as a key event in the pathogenesis of osteoarthritis. Arthritis Rheum 56, 2663–2673.

Yoda M, Kimura T, Tohmonda T, Morioka H, Matsumoto M, Okada Y, Toyama Y, Horiuchi K (2013). Systemic overexpression of TNFalpha-converting enzyme does not lead to enhanced shedding activity in vivo. PLoS One 8, e54412.